EXAMINATION OF MELATONIN RECEPTOR EXPRESSION IN THE 6-HYDROXYDOPAMINE RAT MODEL OF PARKINSON'S DISEASE

By

Na Hyea Kang, BSc

A Thesis

Submitted to the School of Graduate Studies

In partial fulfillment of the Requirements

For the Degree

Master of Science

McMaster University

MASTER OF SCIENCE (2014)

McMaster Integrative Neuroscience Discovery & Study (MiNDS)

McMaster University

Hamilton, Ontario

TITLE: Examination of melatonin receptor expression in the 6-hydroxydopamine rat model of Parkinson's disease

AUTHOR: Na Hyea Kang, BSc (University of Toronto)

SUPERVISOR: Dr. L. P. Niles

NUMBER OF PAGES: xii, 76

Abstract:

Melatonin has a neuroprotective function, which is mediated via its G-protein-coupled MT_1 and MT_2 receptors. When activated, various downstream pathways are triggered promoting cell protection and survival. By utilizing this function of melatonin, studies have shown positive effects in animal models of neurodegenerative disorders such as Parkinson's disease (PD). In our previous studies, a physiological dose of melatonin was shown to have neuroprotective effects in the nigrostriatal pathway, as indicated by preservation of tyrosine hydroxylase (TH) immunoreactivity in a 6-hydroxydopamine (6-OHDA) model of PD. We also have reported that transplantation of MT_1 receptor-expressing mouse neural stem cells (C17.2) along with melatonin treatment, preserved TH immunoreactivity in a similar PD model. Moreover, others have reported an increase in striatal melatonin levels in 6-OHDA-induced hemiparkinsonian rats. Based on these implications of a close relationship between the dopaminergic and melatonergic systems, we hypothesize that degeneration of dopaminergic neurons induced by 6-OHDA will affect the melatonergic system in the nigrostriatal pathway. In this study, 6-hydroxydopamine was unilaterally injected in the rat striatum or medial forebrain bundle. An apomorphine rotation test showed significant increases in net contralateral rotations ($p<0.01$) in lesioned animals as compared to sham. Also, a loss of TH immunoreactivity in the striatum and substantia nigra was seen in striatum lesioned groups, confirming lesion-induced degeneration of dopaminergic neurons in the nigrostriatal pathway. There were no significant differences in MT_1 receptor protein expression in the striatum and substantia nigra, between all intrastriatal lesioned groups and the sham group. However,

6-OHDA lesions in the medial forebrain bundle caused a significant increase in MT_1 receptor mRNA expression on the lesioned side (right) of the ventral midbrain as compared with the contralateral side. These results suggest that MT_1 receptors are upregulated in the ventral midbrain following lesion-induced dopaminergic neurodegeneration, and may be involved in an endogenous neuroprotective mechanism.

Acknowledgements

I would like to express my deepest appreciation and thanks to my supervisor, Dr. Niles for his tremendous support, inspiring guidance and never-ending encouragement throughout the course of my studies. My experience in the lab as a Master's degree student has been the most valuable experience in my life.

I would also like to thank my committee members, Dr. Foster and Dr. Mishra for their constructive criticism and friendly advice throughout various milestones of this project.

Also, I would like to thank Sarra Bahna and Candace Carriere, my fellow colleagues, for their help toward many successful stereotaxic animal surgeries.

Most importantly, a special thanks to my family and friends for their on-going support and up-lifting my spirits.

Table of Contents

2. METERIALS AND METHODS

List of Figures

List of Abbreviation and Symbols

6-OHDA	6-hydroxydopamine	CYP1A1	Cytochrome p450 1A1
AA-NAT	Arylalkylamine N-Acetyltransferase	CYP1A2	Cytochrome p450 1A2
AC	Adenylate Cyclase	CYP1B	Cytochrome p450 1B
AFMK	N1-Acetyl-N2-formyl-5-methoxylkynuramines	CYP2C19	Cytochrome p450 2C19
AKT	Protein kinase B	D2 receptor	Dopamine receptor 2
AMK	N1-acetyl-5-methoxykynuramine	EDTA	Ethylenediaminetetraacetic acid
cAMP	Cyclic adenosine 3', 5'-monophosphate	ERK 1/2	Extracelluar signal-regulated kinase -1 and -2
cDNA	Complementary DNA	GAPDH	Glyceraldehyde 3-phosphate dehydrogenase
cGMP	Cyclic guanosine 3', 5' monophosphate	GDNF	Glial cell line-derived neurotrophic factor
CHO	Chinese hamster ovary cells	GT1-7	Gonadotropin releasing hormone neuronal cell
CREB	cAMP responsive element binding protein	HCl	Hydrogen chloride

HEK 293	Human embryonic kidney 293 cells	PKA	Protein kinase A
HIOMT	hydroxyindole-O-methyltransferase	PKC	Protein kindase C
i.p	intraperitoneal	PLC	Phopholipase C
Kir3	Inwardly rectifying potassium channels	PMSF	pheylmethylsulphonyl fluoride
MAPK	Mitogen activated protein kinase	PTX	Pertussis toxin
MT1	Melatonin receptor subtype 1	PVDF	Polyvinylidene fluoride
MT2	Melatonin receptor subtype 2	ROS	Reactive oxygen species
NaCl	Sodium chloride	s.c	subcutaneous
NE	Norepinephrine	SCN	suprachiasmatic nucleus
NGF	Nerve growth factor	SDS	Sodium dodecyl sulfate
NSC	Neural stem cell	SNAT	N-acetyltransferase
OD	Optical density	TBST	Tris-Vuffered Saline and Tween 20
PBS	phosphate-buffered saline	TH	Tyrosine hydroxylase
PD	Parkinson's disease		
PFA	Paraformaldehyde		
PI3K	Phophoinositide-3 kinase		

Declaration of Academic Achievement

My supervisor, Dr. Niles, designed the experiments and performed the animal sacrifices as well as brain dissections for mRNA analysis. I performed stereotaxic surgeries as a primary surgeon and carried out behavioural tests. I was also responsible for the animal care. Sarra Bahna and Candace Carriere, fellow graduate students, helped with stereotaxic surgeries as secondary surgeons. I executed all the cellular and molecular procedures including slicing, immunohistochemistry, western blotting, and RT-PCR. With help from Robyn MacKenzie, the lab technician from Dr. Foster's lab, I made the MT_1 riboprobe for *in situ* hybridization. Dr. Foster performed the *in situ* hybridization procedure.

1. Introduction

1.1 Melatonin

Melatonin (5-methoxy-N-acetyltryptamine), also known as the 'hormone of darkness,' is secreted primarily by the pineal gland. As implied by its nickname, the secretion level peaks during the dark period of the daily light/dark cycle. The rhythmicity of melatonin secretion conveys daily light/dark cycles, as well as seasonal cycle information to all tissues. Hence melatonin is considered a chronological pacemaker or 'Zeitgeber' (Pandi-Perumal et al., 2006). In addition to relaying the circadian rhythm information, melatonin modulates various biological functions including neuroendocrine and immune function, seasonal reproduction, and body temperature (Jimenez-Jorge et al., 2005; Moriya et al., 2007). Also, melatonin has a hypnotic effect as it promotes sleep in diurnal animals (Zhdanova, 2005), inhibits dopamine release in retina (Dubocovich, 1983) and regulates vasoregulatory activity (Doolen et al., 1998; Ting et al., 1999).

1.2 Melatonin: Synthesis

Melatonin synthesis in the pineal gland, involves the uptake of L-tryptophan, a serotonin precursor, which is taken up from blood circulation and converted into 5-hydroxytryptophan by tryptophan hydroxylase. 5-Hydroxytryptophan is subsequently converted into serotonin by aromatic L-amino acid decarboxylase. With signals from retinohypothalamic pathway, serotonin is then acetylated by serotonin N-acetyltransferase (SNAT) or Arylalkylamine N-acetyltransferase (AA-NAT), to produce N-acetylserotonin, a rate-limiting enzyme for the melatonin synthesis (Ganguly et al., 2002). A methyl

group is then transferred from (s)-adenosylmethionine to N-acetylserotonin by hydroxyindole-O-methyltransferase (HIOMT) which results in the final product, melatonin (Dubocovich et al., 2010). Synthesized melatonin is not stored in the pineal gland, but released into the bloodstream and the cerebrospinal fluid (Tricoire et al., 2003). Melatonin is also synthesized in other cells and tissues including the retina, skin, immune and hematopoetic cells, gastrointestinal tract, some reproductive organs and endocrine glands (Luchetti et al., 2010; Pandi-Perumal et al., 2006; Singh & Jadhav, 2014). Although the melatonin concentration in some of these tissues is higher than the plasma level, it is poorly secreted into blood circulation (Hardeland, 2008).

1.3 Melatonin: Regulation

The biosynthesis of the pineal melatonin is controlled by the retinohypothalamic pathway (Pandi-Perumal et al., 2006). The environmental light/dark information is sensed by a small subset of the retinal ganglion cells that carry a photopigment called melanopsin (Berson et al., 2002). Melanopsin is most sensitive to blue light and allows the retinal ganglion cells to be photosensitive, independent of the photoreceptors (Hankins et al., 2008). The sensed photic information from these retinal ganglion cells is relayed to suprachiasmatic nucleus (SCN), which is located in the anterior part of the hypothalamus, and directly above the optic chiasm (Gillette & Mitchell, 2002). Suprachiasmatic nucleus, the master pacemaker of the circadian rhythm, projects descending fibers through the paraventricular nucleus, medial forebrain bundle and reticular formation, which synapse onto intermediolateral horn cells of the spinal cord (Pandi-Perumal et al., 2006). Then the

preganglionic sympathetic fibers innervate the superior cervical ganglion and the postganglionic sympathetic fibers synapse on the pinealocytes. Norepinephrine (NE), released from the postganglionic sympathetic fibers, regulates the melatonin synthesis. During the dark period of the daily light/dark cycle, the SCN activity is inhibited thus leading to an increase in NE release (Pandi-Perumal et al., 2006). When NE binds to the β-adrenergic receptors on the pinealocyte, adenylate cyclase (AC) is activated which leads to an increase in cAMP. cAMP triggers the de novo synthesis of the melatonin synthesizing enzyme, AA-NAT (Claustrat et al., 2005). During the light period of the daily light/dark cycle, SCN activity is high which results in low NE secretion (Pandi-Perumal et al., 2006). Subsequently, synthesis and activation of melatonin synthesizing enzymes is reduced which ultimately leads to a decrease in melatonin synthesis (Pandi-Perumal et al., 2006).

1.4 Melatonin: Metabolism

Most of the circulating melatonin (around 92-97%) is metabolized in the liver in a single pass (Dubocovich et al., 2010). In liver, there are isoenzymes of cytochrome p450 monooxygenases, which metabolize melatonin. CYP1A2, CYP1A1 and CYP1B hydroxylate melatonin in the C6 position, producing 6-hydroxymelatonin (Pandi-Perumal et al., 2006). 6-hydroxymelatonin is conjugated with sulfate and 50-80% gets excreted as 6-sulfatoxymelatonin, and 5-30% gets excreted as the glucoronide into urine (Dubocovich et al., 2010; Hardeland, 2008). Another isoenzyme of cytochrome p450 monooxygenases, CYP2C19, demethylates melatonin to produce N-acetylserotonin, which is a precursor of

melatonin (Hardeland, 2008; Pandi-Perumal et al., 2006). When melatonin is injected directly into the cisterna magna where cerebrospinal fluid is drained from the forth ventricle, 6-hydroxymelatonin was not detected (Dubocovich et al., 2003). In the brain, a considerable amount of melatonin is metabolized into kynuramine derivatives, N1-acetyl-N2-formyl-5-methoxylkynuramines (AFMK) and N1-acetyl-5-methoxykynuramine (AMK), by oxidative pyrrole-ring cleavage route (Dubocovich et al., 2010). AFMK is formed from melatonin by numerous reactions: enzymatic such as indoleamine 2,3-dioxygenase or myeloperoxidase; pseudoemzymatic such as oxoferryl hemoglobin or hemin; photocatalytic and free radical reactions (Hardeland, 2008). AFMK is then deformylated to AMK by arylamine formidase and hemoperoxidase (Dubocovich et al., 2010). Moreover, in the pineal gland and retina, melatonin is deacetylated by melatonin deacetylase or aryl acrylamidase to 5-metoxytrypamine, which is a substrate for monoamine oxidase A (Hardeland, 2008; Pandi-Perumal et al., 2006). Also, melatonin can directly be metabolized by free radicals to either cyclic 3-hydroxymelatonin, which is converted into AFMK or 2-hydroxylated analog, which is further converted into indolione (Hardeland, 2008).

1.5 Melatonin Receptors: MT_1 and MT_2

In mammals, two membrane-bound receptors, known as MT_1 and MT_2 have been identified. Both receptors belong to the G-protein coupled receptor superfamily and consist of seven transmembrane domains with the N-terminus at the extracellular side and C-terminus at the intracellular side (Dubocovich et al., 2010). The MT_1 receptor is

composed of 350 amino acids and has the molecular weight of 39 kDa (Dubocovich et al., 2010). The MT_2 receptor, which is 60% homologous to the MT_1 receptor, is composed of 362 amino acids and has a molecular weight of 40 kDa (Dubocovich et al., 2010). Both receptors have a high binding affinity for melatonin: K_d =20-40pmol/l for human MT_1 receptor and K_d = 160pmol/l for the human MT_2 receptor (Pandi-Perumal et al., 2008). The binding site for these receptors is located on the extracellular side of the fifth transmembrane domain (Dubocovich et al., 2010; Luchetti et al., 2010). There is an additional melatonin binding site with lower affinity, which was initially called MT_3 receptor, but it was later termed as quinone reductase 2 (Nosjean et al., 2000).

MT_1 and MT_2 receptors are expressed in areas of the central nervous system and peripheral tissues. Studies have shown expression of both receptors in retina, hypothalamus, choroid plexus, hippocampus, striatum, substantia nigra, ventral tegmental area, cerebral cortex, cerebellum, kidney, cardiovascular system and immune system (Dubocovich et al., 2010; Hardeland, 2008; Singh & Jadhav, 2014). MT_1 receptor is also expressed in testes, ovary, and adrenal cortex (Dubocovich et al., 2010; Singh & Jadhav, 2014). Various localizations of these receptors suggest that they can exert numerous physiological effects. For instance, MT_1 receptor activation can modulate neuronal firing (Liu et al., 1997), induce vasoconstriction (Ting et al., 1999), reproductive and metabolic functions (Dubocovich et al., 2010; von Gall et al. 2002). MT_2 receptor activation can inhibit dopamine release in retina (Dubocovich, 1983), vasodilation (Doolen et al., 1998),

phase shift circadian rhythms of neuronal firing in the SCN (Dubocovich & Markowska, 2005) and enhance immune response (Drazen & Nelson, 2001).

1.6 Melatonin Receptors: Signal Pathways

MT_1 and MT_2 receptors are coupled with G-proteins, which are composed of α, β, and γ subunits. When melatonin is bound, α and βγ dimer subunits dissociates from the receptor, triggering a cascade of signal transductions. MT_1 receptor can couple to pertussis toxin (PTX)-sensitive G_i and PTX-insensitive G_q proteins, which trigger different signal pathways (Dubocovich et al., 2010). $G\alpha_i$ subunit inhibits activity of adenylyl cyclase reducing forskolin-stimulated cAMP formation (Reppert et al., 1995). Consequently, the reduction of forskolin stimulated cAMP leads to a decrease in the activity of protein kinase A (PKA), thus inhibiting phosphorylation of the cAMP responsive element binding protein (CREB) (Witt-Enderby et al., 1998). Suppression of PKA activity also leads to the activation of the mitogen activated protein kinase/extracellular signal-regulated kinase -1 and -2 (MAPK/ERK1/2) pathway (Witt-Enderby et al., 2000) and the phosphoionositide-3 kinase/protein kinase B (PI3K/AKT) pathway (Koh, 2008; Luchetti et al., 2010). In addition, the MT_1 receptor can increase phospholipase C (PLC) activity (McArthur et al., 1997) and activate inwardly rectifying potassium channels (Kir3) by βγ dimer subunit of the pertussis toxin sensitive G proteins (Jiang et al., 1995).

Similarly, activation of MT_2 receptors can also bind to multiple G-proteins including $G\alpha_i$ and $G\alpha_q$ proteins. Activation of MT_2 triggers inhibition of adenylyl cyclase and guanylyl cyclase, which results in reduced cAMP and cGMP formation (Petit et al., 1999; Reppert et al., 1995). It can also trigger activation of PLC resulting in an increase production of phophoinositide and diacylglycerol, which leads to an increase in protein kinase C (PKC) activity (McArthur et al., 1997). The phase shifting effect of the SCN circadian clock is modulated by the activation of the PKC activity (Hunt et al., 2001).

1.7 Melatonin Receptors: Regulation

A high level of melatonin synthesis persists during the dark period of the daily circadian cycle. This prolonged period of melatonin exposure is thought to have a desensitization effect on melatonin receptors, which is essential to maintain the cellular homeostasis. Moreover, studies have shown an inverse relationship between the rhythmicity of melatonin synthesis and the density of melatonin receptors in SCN and pars tuberalis (Gauer et al., 1993; Tenn & Niles, 1993), suggesting involvement of a desensitization mechanism. Prolonged exposure to melatonin leads to changes in its receptor sensitivity, which may involve G protein uncoupling, internalization, or down-regulation (Ferguson, 2001; Witt-Enderby et al., 2003). The MT_1 receptor in Chinese hamster ovary (CHO) cells showed an increase in uncoupled heterotrimeric G proteins after the prolonged melatonin exposure, thus leading to a decrease in the efficacy of melatonin binding at the receptor (Witt-Enderby et al., 2003). Also, after short-term exposure to melatonin, arrestin-dependent internalization of MT_1 and MT_2 receptors was

observed in GT1-7 neurons and in CHO cells respectively (Gerdin et al., 2003; Roy et al., 2001). Furthermore, melatonin receptor was functionally desensitized following an exposure to melatonin as indicated by an inhibition of receptor-mediated forskolin-induced cAMP production and phophoinositide hydrolysis (MacKenzie et al., 2002).

1.8 Melatonin and Melatonin Receptors: Neuroprotection

The neuroprotective effects of melatonin are thought to involve its antioxidative property, hence reducing the oxidative stress in neurons. At high pharmacological doses, melatonin will enhance antioxidant activity by directly scavenging free radicals (Mayo et al., 2002; Sharma et al., 2006), whereas at physiological doses, it induces the expression of antioxidant enzymes (Mayo et al., 2002; Rodriguez et al., 2004). Also, the neuroprotective effect of melatonin can be mediated by MT_1 and MT_2 receptors. Binding of melatonin to its receptors triggers various downstream pathways including PI3K/AKT and MAPK/ERK, which promote cell protection and survival (Koh, 2008; Luchetti et al., 2010). Furthermore, the neuroprotective effects of melatonin can be exerted by modulating the expression of neurotrophic factors. Melatonin, at a physiological concentration, increases nerve growth factor (NGF) in the mouse submandibular gland (Pongsa-Asawapaiboon et al., 1998). Intrastriatal melatonin injection elevates glial cell line-derived neurotrophic factor (GDNF) mRNA in the rat striatum (Tang et al., 1998). We have reported that melatonin treatment in physiological concentrations up-regulate GDNF mRNA expression in rat C6 glioma cells (Armstrong & Niles, 2002). Similarly, physiological melatonin treatment increased GDNF mRNA expression in MT_1 receptor –

expressing C17.2 mouse neural stem cell (Niles et al., 2004). Thus, these results suggest that melatonin can exert both direct and indirect roles in neuroprotection. It is well established that the overall melatonin biosynthesis declines as we age, which suggests vulnerability and acceleration of damage to neurons, an implication for age-related neurodegeneration, such as Parkinson's disease (Karasek, 2004; Mishima et al., 2001).

1.9 Parkinson's Disease

Parkinson's disease is one of the common neurodegenerative disorders, which results in motor impairments including bradykinesia, rigidity, resting tremor and postural instability. One of the key hallmarks of Parkinson's disease is a progressive loss of dopamine neurons in the substantia nigra with an associated decrease of dopaminergic function in the striatum. Other characteristics of Parkinson's disease include gliosis and Lewy body aggregates in dopaminergic neurons (Bove et al., 2005). The etiology of PD still remains unclear but studies have shown that the production of reactive oxygen species (ROS), by mitochondrial impairment and dopamine metabolism, play a crucial role in the degeneration of dopaminergic neurons (Mayo et al., 2005).

1.10 6-hydroxydopamine

6-hydroxydopamine is a neurotoxic metabolite of dopamine that is detected in the Parkinson's disease patient's brain and urine (Gomez-Lazaro et al., 2008). It is known to selectively destroy catecholamine neurotransmitter neurons when administered in certain areas of the brain (Gomez-Lazaro et al., 2008). Due to its similar molecular structure to

dopamine and norepinephrine, it has a high affinity to bind to dopamine and norepinephrine transporters, allowing it to easily enter dopamine and norepinephrine neurons (Bove et al., 2005). When 6-hydroxydopamine is injected into the nigrostriatal pathway along with i.p. injection of desipramine (a drug that inhibits norepinephrine reuptake), it specifically damages dopaminergic neurons. The mechanism of 6-hydroxydopamine-induced neurodegeneration has not been fully understood, but studies have shown that reactive oxygen species and *para*-quinones, resulting from oxidation of 6-hydroxydopamine, as well as inhibition of mitochondrial function, lead to dopaminergic neuronal injury and eventually neuronal death (Simola et al., 2007). In addition to loss of dopaminergic neurons, which is a key biochemical hallmark for Parkinson's disease, the injection of 6-hydroxydopamine in the nigrostriatal pathway causes reactive gliosis, which is also one of the neuropathological features of Parkison's disease (Bove et al., 2005). Hence, 6-hydroxydopamine has been a popular tool to generate animal models of Parkinson's disease.

1.11 Melatonin and the Dopaminergic System

Various studies have shown an interaction between melatonin and dopamine in the nigrostriatal pathway. Hamdi (1998) reported that chronic melatonin treatment increases the affinity (as shown by a decrease in K_d) of the D2 receptor in rat striatum, allowing dopamine to easily bind to its receptor and presumably enhancing dopaminergic function. There is also evidence that chronic administration of melatonin causes a significant increase in the mRNA expression of tyrosine hydroxylase (TH), the rate-

limiting enzyme for dopamine synthesis, in the rat substantia nigra and ventral tegmental areas (Venero et al., 2002). We have reported that chronic treatment with a physiological dose of melatonin is neuroprotective for dopaminergic neurons, as indicated by the preservation of TH immunoreactivity, in an animal model of Parkinson's disease (Sharma et al., 2006). Furthermore, transplantation of MT_1 receptor-expressing mouse neural stem cells (C17.2) along with melatonin treatment, preserved TH immunoreactivity in rats that were intrastriatally lesioned with 6-hydroxydopamine (Sharma et al., 2007). Physiological doses (nanomolar range) of melatonin were shown to increase TH protein expression in human SH-SY5Y neuroblastoma cells, following retinoic acid-induced differentiation into dopamine neurons (McMillan et al., 2007). These studies suggest an intimate relationship between the melatonergic and dopaminergic systems.

1.12 Hypothesis

Based on the above findings, we postulate that degeneration of dopaminergic neurons, induced by 6-hydroxydopamine, will alter melatonin receptor expression in the nigrostriatal pathway.

1.13 Objectives

a) To determine whether melatonin receptor MT_1 and/or MT_2 expression levels are altered after intrastriatal 6-hydroxydopamine lesions in rats.
b) To determine whether melatonin receptor MT_1 and/or MT_2 expression levels are altered after 6-hydroxydopamine lesions of the medial forebrain bundle in rats.

2. Materials and Methods

2.1 Unilateral intrastriatal 6-hydroxydopamine lesions

2.1.1 Animals

Adult male Sprague-Dawley rats weighing 350-375g at the beginning of the experiment were used. All animals were housed under 12 hour light/dark cycle with lights on at 7am. They were kept at an ambient temperature with free access to regular food and water. All experiments were carried out according to the guidelines set by the McMaster University Animal Research Ethics Board (AREB).

2.1.2 6-Hydroxydopamine Lesions

Lesioning was carried out as we have previously reported (Sharma et al., 2006) Fifteen minutes prior to surgery, animals were injected (i.p.) with 15mg/kg desipramine. Animals were anesthetized using isofluorane gas (5% in O_2 for induction, 2.5% in O_2 for maintenance) and secured in a Kopf stereotaxic apparatus with the incisor bar set 3 mm above the interaural line. Secured animals were then injected (s.c) with ketoprofen (10mg/kg) and saline (5 ml). Animals were randomly divided into sham, lesioned with 8.75 µg of 6-hydroxydopamine, 16 µg of 6-hydroxydopamine or 20 µg of 6-hydroxydopamine. These three different amounts of 6-hydroxydopamine were prepared in 4 µl of 0.1% ascorbic acid. The neurotoxin was unilaterally injected into the right striatum (AP, 1.0 mm; LM, -2.8 mm; DV, -5.6 mm from Bregma) using a Hamilton syringe at an infusion rate of 1 µl/min and the needle was left in place for 5 min to allow

diffusion. Sham animals were injected with the vehicle (4µl of 0.1% ascorbic acid in saline) in the same manner. Enrofloxacin (5-10 mg/kg) was injected (i.m) after surgery.

2.1.3 Behavioural testing

At two weeks post-surgery, a forelimb asymmetry test was performed to examine the change in motor functions. Each week until the sacrifice, animals were placed in a clear plexiglass cylinder (23 cm diameter, 35 cm depth) for 5 min under red light during the dark cycle. The total number of rears, and right or left forelimb contacts on the cylinder wall were recorded for data analysis.

An apomorphine rotational test was also performed at three weeks post-surgery between 1 PM to 3 PM. All animals were injected (s.c.) with apomorphine hydrochloride (0.25mg/kg) in saline. After a 5-min waiting period in their home cages, the animals were placed in a metal bucket (28 cm diameter, 35 cm depth) and rotations were counted for 10 min.

2.1.4 Tissue collection

Eight weeks post- surgery, one animal from each group was transcardially perfused with saline followed by 4% paraformaldehyde (PFA) for subsequent tyrosine hydroxylase immunohistochemistry. Harvested whole brains were post-fixed in 4% PFA at 4°C overnight and then cryoprotected in 30% sucrose at 4°C for 3 days. Cryoprotected brains were then stored in -80°C.

Rest of the animals were quickly decapitated between hours of 11 AM and 2 PM. Whole brain tissues were harvested rapidly on ice then flash frozen in the pre-chilled ethanol on dry ice. All harvested brains were then stored in -80°C until further analysis.

2.1.5 Tyrosine hydroxylase Immunohistochemistry

Perfused brains were coronally sliced (35 μm in thickness) by cryostat at -20°C. 1 in 10 striatal and substantia nigral slices were collected in 1X PBS solution, beginning at approximately 2.0 mm relative to Bregma for striatal slices and approximately – 4.8 mm relative to Bregma for substantia nigral slices. Free-floating slices were incubated in polyclonal anti-tyrosine hydroxylase (1:400) at 4°C overnight and then incubated with FITC-conjugated donkey anti-rabbit IgG (1:200) for 2 hours at room temperature. The images of the slices were captured with Zeiss LSM510 confocal microscope.

2.1.6 Riboprobe

Complimentary DNA (cDNA) for MT_1 was produced by polymerase chain reaction (MT_2: (f)tacatcagcctcatctggctt (r)cacaaacactgcgaacatggt (297bp), MT_1: (f)agcttgtcaacgcctctcag (r)tcaggaacacgtagcacagg (441bp)). The amplified product was run on agarose gel electrophoresis to obtain purified and desired size of the cDNA. Excised gel with was cleaned to recover the cDNA using gel extraction kit (Qiagen, Mississauga, ON, Canada). Purified cDNA was ligated into the pGEM T-easy expression vector (Promega, Mississauga, ON, Canada) and transformed into DH5α competent cells (Invitrogen, Burlington, ON, Canada). Plasmid DNA was harvested by maxiprep kit

(Qiagen, Mississauga, ON, Canada) and then sequenced (Mobix Lab, McMaster University). Using NCBI Blast tool, sequence was blasted to confirm the specificity of the riboprobe for MT_1. Antisense and sense probes were transcribed using α-^{35}S-UTP (specific activity>1000C_i/mmol; Perkin-Elmer, Boston, MA) with T7 and SP6RNA polymerase. No signal was detected for sense probes.

2.1.7 In Situ Hybridization

In situ hybridization procedures were performed as previously reported (Bahna et al., 2014). Thaw-mounted brain sections were fixed with 4% formaldehyde then acetylated with 0.25% acetic anhydride in 0.1M triethanolamine-HCl, pH 8.0. Brain sections were then dehydrated and delipidated with chloroform. The brain sections were incubation in a hybridization buffer with radiolabeled probes. Following overnight incubation at 55°C in a humidified chamber, slides were washed in 20µg/ml RNase solution for 30 min to minimize nonspecific binding of probes. Slides were then washed in 2X SSC at 50°C for 1 hour, 0.2X SSC at 55°C and 60°C. Subsequently, slides were dehydrated and air-dried for autoradiography.

2.1.8 Western Blot of MT_1 protein expression

Flash frozen whole brains were slightly thawed on ice and coronally sliced in 2mm intervals using a rat brain matrix. Striatum, hippocampus, substantia nigra, hypothalamus and cerebellum were then teased out from the coronal slices. Proteins were extracted from the dissected tissues using lysis buffer (50mM Tris-HCl, 150mM NaCl,

1mM EDTA, 1% Triton X-100, 1mM phenylmethylsulphonyl fluoride (PMSF), and Roche protease inhibitor cocktail). Other lysis buffers were tried for optimization which are: Standard: 50 mM Tris-HCl, 150 mM NaCl, 1mM EDTA, 1% Triton X-100, 1mM PMSF and Roche protease inhibitor cocktail mix. 'a': 50 mM Tris-HCl pH 7.4, 150 mM NaCl, 1 mM EDTA, 1% NP-40, 0.25% sodium deoxycholate, 1mM PMSF, sodium orthovanadate (2 mM) and Roche protease inhibitor cocktail mix (Castro et al., 2005). 'b': 20mM Tris-HCl, 150mM NaCl, 1mM EDTA, 1mM EGTA, 2.5mM sodium pyrophosphate, 1mM b-glycerophosphate, 1mM sodium orthovanadate, 0.01% Triton X-100, 0.01% NP-40, Roche protease inhibitor cocktail mix (Wang et al., 2012). 50 µg of proteins were loaded on to a 12% SDS-Polyacrylamide gel. Gels were run at 200V for an hour in 4°C then transferred to PVDF membrane at 100V for an hour in 4°C. Blots were blocked with 5% non-fat dry milk in TBST buffer for 1 hour at room temperature and then incubated overnight in rabbit anti-MT_1 antibody (1:1000) at 4°C. Subsequently, MT_2 blots were incubated in anti-rabbit horseradish peroxidase-conjugated antibody (1:5000) for 2 hours at room temperature, then treated with enhanced chemiluminesence reagent for 5 min. Blots were exposed onto film to detect proteins then stripped and re-probed with anti-ß-actin (1:5000) as the internal standard.

2.1.9 Data Analysis

Films were digitally scanned and the optical density (OD) values of protein bands were measured using the AlphaImager 2200 program. The OD ratios, MT_1 protein

expression levels over internal standard (ß-actin) were obtained for semi-quantitative analysis.

2.2 6-Hydroxydopamine lesions of medial forebrain bundle

2.2.1 Animals

Adult male Sprague-Dawley rats weighing 350-380g at the beginning of the experiment were used. All animals were housed under 12 hour light/dark cycle with lights on at 7am. They were kept at an ambient temperature with free access to regular food and water. All experiments were carried out according to the guidelines set by the McMaster University Animal Research Ethics Board (AREB).

2.2.2 6-Hydroxydopamine Lesions

Surgery was carried out in the same manner as mentioned above. Animals were randomly divided into sham and lesioned groups and desipramine injection was omitted. Two unilateral injection sites in the right medial forebrain regions were selected (AP, -4.0 mm; ML, -0.8 mm; DV, -8.0 mm from Bregma, incisor bar, 3.5mm above the interaural line and AP, -4.4mm; ML, -1.2mm; DV, -7.8mm from Bregma, incisor bar set at the interaural line) (Blandini et al., 2009; Kirik et al., 1998). 9 µg of 6-OHDA for the first site and 7.5 µg 6-OHDA for the second site were prepared in 3 µl of 0.02% ascorbic acid and injected using a Hamilton syringe at an infusion rate of 1 µl/min and the needle was left in place for 5 min for diffusion. Sham animals were injected with the vehicle (3 µl of

0.02% ascorbic acid in saline) in the same manner. Enrofloxacin (5-10 mg/kg) was injected (i.m) after surgery.

2.2.3 Behavioural testing

Apomorphine-induced rotational behaviour was examined at three weeks post-surgery between 1 PM to 3 PM. All animals were injected (s.c.) with apomorphine hydrochloride (0.25mg/kg), prepared in saline. After a 5-min of waiting period in their home cages, the animals were placed in a metal bucket (28 cm diameter, 35 cm depth) and rotations were counted for 10 min.

2.2.4 Tissue collection

Four weeks post-surgery, three sham animals and six lesioned animals were randomly selected for decapitation between hours of 11 AM and 2 PM. Various brain regions (frontal cortex, striatum, hippocampus, ventral midbrain, hypothalamus, cerebellum) were quickly dissected from each hemisphere of the brain and stored in RNALater at 4°C until RNA extraction.

2.2.5 RT-PCR detection

RNALater was discarded and the dissected tissues were weighed. Total RNA was extracted using 1ml of TRIzol reagent per ≤ 50 mg of homogenized tissue, as detailed by the supplier (Life technologies, Burlington, ON). Subsequently, DNAse treatment was performed with 5-15µg of total RNA. Complementary DNA (cDNA) was synthesized

from the concentration-adjusted amount of DNAsed treated RNA using the Omniscript reverse transcriptase kit (Qiagen Inc., Mississauga, ON) and oligo DT primers. 10µl of cDNA was amplified with rat MT_1 receptor primers (f)agcttgtcaacgcctctcag (r)tcaggaacacgtagcacagg (441bp) and HotStarTaq master mix kit (Qiagen Inc., Mississauga, ON) by using the following PCR parameters: 94°C for 30s, 57°C for 30s and 72°C for 1min for 40 cycles followed by a final incubation at 72°C for 10min.

2.2.6 Data analysis

Amplified cDNA samples were run on 1.5% agarose gels, stained with ethidium bromide and visualized under UV light. Optical density (OD) values were obtained from digitally scanned gel images using the AlphaImager 2200 program. The OD ratios, MT_1 mRNA expression level over internal housekeeping gene (GAPDH), were obtained for semi-quantitative analysis.

2.3 Statistical analysis

Rotational data were analyzed by one-way analysis of variance (ANOVA) and group differences determined by a Newman–Keuls test. Behavioural (asymmetrical) data were analyzed by a two-way ANOVA (treatment x time) and significant group differences were determined by a Bonferroni test (Graphpad Prism version 4.0).

Optical density ratios from westerns and RT-PCR analyses were converted to percentage values relative to controls, followed by ANOVA and Unpaired Student's test, respectively. Data are presented as means ± S.E.M. and considered significant when $p < 0.05$.

3. Results

3.1 Unilateral intrastriatal 6-hydroxydopamine lesions

3.1.1 Effects of unilateral intrastriatal 6-hydroxydopamine injections on rat health

23 out of 24 animals survived stereotaxic surgery. All surviving animals (both lesioned and sham groups) fully recovered from surgery and maintained good health. There were no significant differences in body weight between groups (Fig 1A).

3.1.2 Forelimb asymmetry test

At 2 weeks post-surgery, the asymmetry test was started during the dark phase of the circadian cycle, when the rats are most active. At 7 weeks post-surgery, two-way ANOVA followed by Bonferroni post-hoc test showed a significant ($p < 0.01$) decrease in left forelimb usage in medium dose (16 µg 6-OHDA) and high dose (20 µg 6-OHDA) lesioned groups as compared to sham group (Fig 2B). A decrease in left forelimb use was also observed in the high dose (20 µg 6-OHDA) lesioned group at earlier times, but no group differences were found, probably due to the high variance in data. There were no significant differences in right forelimb usage between any groups (Fig 2A).

3.1.3 Rotational behaviour

At 3 weeks post-surgery, apomorphine, a dopamine agonist, was subcutaneously injected into all animal groups and net rotations were observed. The mean for net rotations per 10 min were 1.25 ± 0.57 ($n = 6$) for the sham group, 30.21 ± 8.59 ($n = 5$) for the low dose (8.75 µg 6-OHDA) lesioned group, 39.77 ± 7.55 ($n = 5$) for the medium

dose (16 μg 6-OHDA) lesioned group, and 37 ± 6.68 (n = 5) for the high dose (20 μg 6-OHDA) lesioned group. Newman-Keuls test indicated a significant ($p<0.01$) increase in apomorphine-induced net contralateral rotations in all lesioned groups as compared to sham group (Fig 3A).

3.1.4 Tyrosine Hydroxylase immunohistochemistry

At 8 weeks post-surgery, one animal from each group was selected and transcardially perfused in 4% paraformaldehyde to test the TH immunoreactivity in the striatum and substantia nigra. There was an apparent reduction in TH immunoreactivity on the lesioned side of the striatum and substantia nigra across all lesioned groups as compared to the sham group (Fig 4 and Fig 5). The TH immunoreactivity of the lesioned striatum was visibly lower in the medium and the high doses of 6-OHDA lesioned groups as compared to the low dose of 6-OHDA lesioned group. There were no visible differences observed in TH immunoreactivity of the lesioned substantia nigra between lesioned groups. Also, there were no changes in TH immunoreactivity in the contralateral striatum or substantia nigra of any groups.

3.1.5 *in situ* hybridization

There was no signal observed for MT_1 and MT_2 probes in the striatum, hippocampus, and substantia nigra. This procedure will be attempted again in the future using probes with higher specific activity and longer exposure times.

3.1.6 MT_1 Western blot protocol optimization

Two non-lesioned rats were decapitated, and harvested brains were snap frozen by ethanol or 2-methylbutane to test the effectiveness of protein preservation. Protein was extracted from the dissected striatum from both brains and tested for tyrosine hydroxylase. As shown on Fig 6, both 2-methylbutane snap frozen tissues and ethanol snap frozen tissues were able to detect TH protein level.

Additional brain regions (substantia nigra & ventral tagmental area and hypothalamus) were dissected from the ethanol snap frozen brain. Various protein amounts of striatum (25 μg, 50 μg) and substantia nigra (20 μg, 50 μg, and 75 μg) were tested with the MT_1 antibody to determine optimal amount of protein for the western blot protocol. The anticipated MT_1 receptor bands (around 39 kDa) were seen in all protein amounts of both tissues (Fig 7A). The best result was obtained with 50 μg of striatum and substantia nigra. In addition, primary MT_1 antibody was incubated for 24 hours and 72 hours to determine the optimal incubation time (Fig 7B and C). 24-hours primary antibody incubation was sufficient to detect MT_1 protein expression whereas 72-hours incubation showed oversaturated bands. All MT_1 protein blots showed multiple non-specific bands. To optimize protein extraction and to possibly eliminate non-specific bindings, different lysis buffers were tested. As shown in Fig 7D, there were no apparent differences between the standard and the 'a' lysis buffer. The 'b' lysis buffer eliminated some non-specific bands, but didn't detect anticipated MT_1 protein band. Lastly, the primary antibody was omitted in the protocol to examine possible non-specific binding of

the secondary antibody. No bands were detected (blots not shown) when the primary antibody was omitted.

3.1.7 Validation of MT_1 primary antibody specificity

To investigate the specificity of the antibody, a blocking peptide (offered by the same company which supplied the primary antibody) was utilized as a negative control. The MT_1 antibody was pre-incubated overnight with the blocking peptide (100x concentrated than the MT_1 antibody) to block the MT_1 specific binding sites. The anticipated MT_1 bands were still detected on the blocked antibody blot (Fig 8A). Moreover, formerly prepared MT_1 antibody (different lot numbered) by the same company was tested but no bands were observed in the non-blocked antibody blot as well as the blocked antibody blot (Fig 8B).

As for the positive control, additional brain regions (hippocampus, cerebellum, and hypothalamus), which are known to express MT_1 receptor, were dissected from the ethanol-frozen brain and tested with the MT_1 antibody. The anticipated MT_1 bands as well as non-specific bands were observed in all additional brain regions (Fig 8C). The highest protein expression level was detected in hypothalamus and cerebellum.

Further investigation on the specificity of the MT_1 antibody was performed *in vitro*. C17.2 mouse neural stem cells (NSCs) and C6 rat glioma cells, which are also known to express MT_1 receptor, were selected as positive controls (Castro et al., 2005; Niles et al., 2004). A single band around 30 kDa was detected in C17.2 mouse NSCs (Fig 9A). C6 cells showed the anticipated MT_1 band around 39 kDa and multiple non-specific

bands as seen in rat brain tissues (Fig 9B). HEK 293 cells, which lack MT_1 receptor, were selected as an *in vitro* negative control. There were no anticipated MT_1 band or non-specific bands were observed on the blot.

3.1.8 MT_1 protein expression

Striatum and substantia nigra were dissected out from each cerebral hemisphere of the ethanol-frozen brains, which was preserved after 8 weeks post-surgery. Dissected tissues were then tested for MT_1 protein expression level. There were no significant changes of MT_1 protein expression level in lesioned or intact striatum (n=3) and substantia nigra (n=3) between the control and lesioned groups (Fig 10 and 11).

3.2 6-Hydroxydopamine lesions of medial forebrain bundle

3.2.1 Effects of unilateral 6-hydroxydopamine injections in the medial forebrain bundle on rat health

21 out of 25 animals survived the stereotaxic surgery. All surviving animals (both lesioned and sham groups) fully recovered from the surgery and maintained good health. There were no significant differences in body weight between groups (Fig 1B).

3.2.2 Rotational behaviour

At 3 weeks post-surgery, apomorphine was subcutaneously injected into all animal groups and net rotations were observed for 10 min. The mean net rotations were 3.63 ± 1.18 (n = 7) for the sham group, and 72.45 ± 9.45 (n = 14) for the lesioned group.

Student's t test revealed a significant ($p<0.0001$) increase in the apomorphine-induced net contralateral rotations in the lesioned group as compared to the sham group (Fig 2B).

3.2.3 MT_1 mRNA expression

Four weeks post-surgery, rats were decapitated and the striatum and ventral midbrain tissues from each hemisphere were collected for RT-PCR analysis (n=3). MT_1 mRNA levels were measured in optical density (OD) values and normalized with a house keeping gene (GAPDH) OD values. The MT_1/GAPDH OD ratio showed a significant ($p<0.03$, Unpaired student's test) increase in MT_1 mRNA expression level in the lesioned side (right) of the ventral midbrain after 6-OHDA lesions in the medial forebrain bundle fibers, as compared with the contralateral (control) side (Fig 12).

Figure 1. Effects of 6-hydroxydopamine intracranial injections on rat weight. A) Animals' weights after unilateral intrastriatal 6-OHDA lesions. Groups: Sham, Low dose (8.75 μg 6-OHDA) lesion, medium dose (16 μg 6-OHDA) lesion, high dose (20 μg 6-OHDA) lesion. No significant difference was seen between any groups (n = 5-6). B) Animals' weights after the 6-OHDA lesions on medial forebrain bundle fibers. No significance was observed between any groups (n = 7-14). Groups: Sham and Lesion.

A)

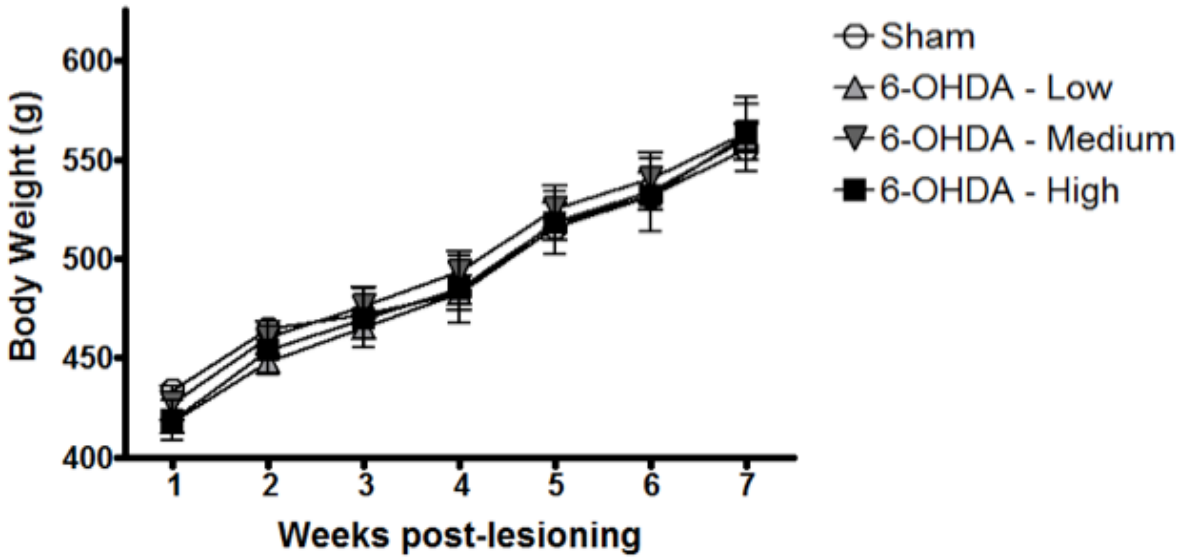
Body Weight (g)
600
550
500
450
400
1
2
3
4
5
6
7
Weeks post-lesioning
Sham
6-OHDA - Low
6-OHDA - Medium
6-OHDA - High

B)

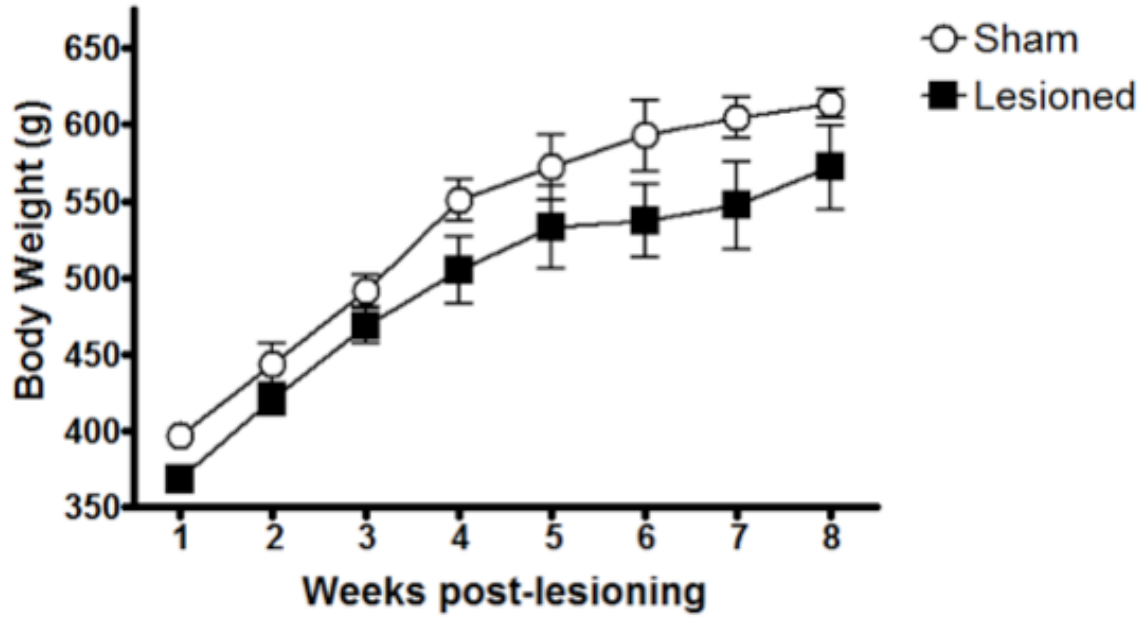
Body Weight (g)
650
600
550
500
450
400
350
1
2
3
4
5
6
7
8
Weeks post-lesioning
Sham
Lesioned

Figure 2. Number of right (A) or left (B) forelimb contacts on the wall of cylinder during the forelimb asymmetry test. Groups: Sham, Low dose (8.75 μg 6-OHDA) lesion, medium dose (16 μg 6-OHDA) lesion, high dose (20 μg 6-OHDA) lesion. Weeks 2-7 indicate the number of weeks post-surgery. Bars represent mean ± S.E.M of forelimb contacts/5min for n=5-6. **P<0.01 versus medium and high doses of 6-OHDA in week 7 (Two-way ANOVA and Bonferroni posttests).

A)

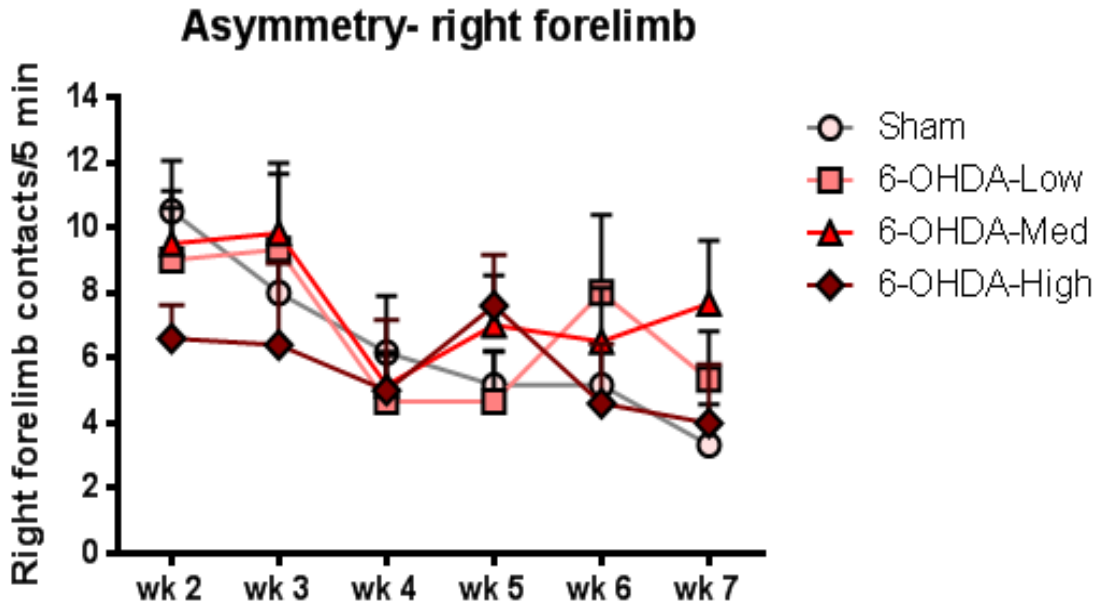
Asymmetry- right forelimb
Right forelimb contacts/5 min
14
12
10
8
6
4
2
0
wk 2
wk 3
wk 4
wk 5
wk 6
wk 7
Sham
6-OHDA-Low
6-OHDA-Med
6-OHDA-High

B)

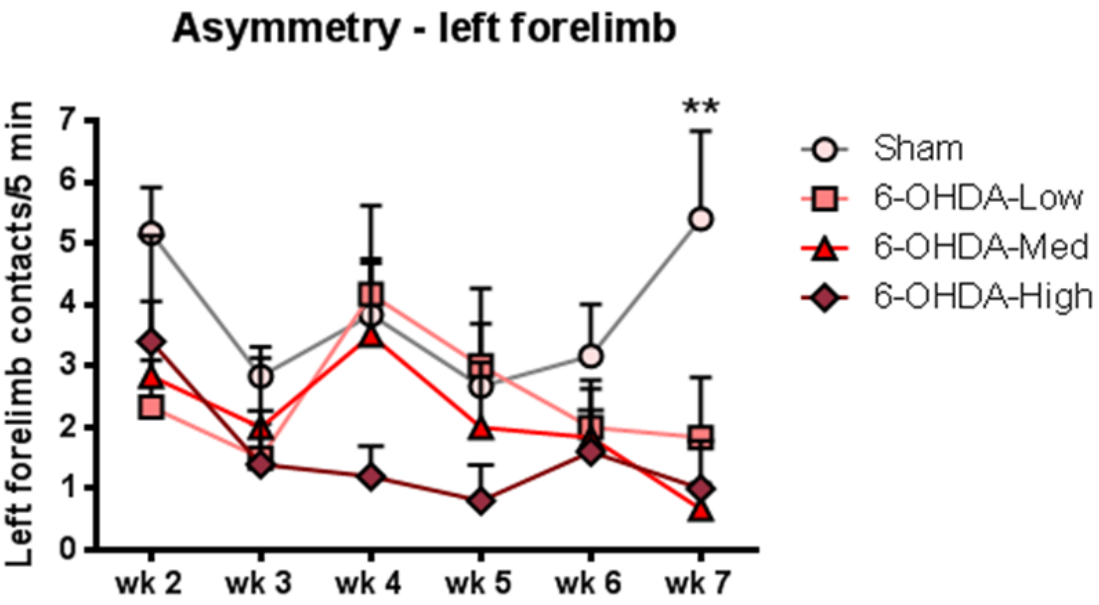
Asymmetry - left forelimb
Left forelimb contacts/5 min
**
7
6
5
4
3
2
1
0
wk 2
wk 3
wk 4
wk 5
wk 6
wk 7
Sham
6-OHDA-Low
6-OHDA-Med
6-OHDA-High

Figure 3. Rotational behaviour induced by apomorphine injection in lesioned animals. A) Apomorphine-induced rotational behaviour in animals lesioned in striatum with 6-hydroxydopamine. Groups: Sham, Low dose (8.75 μg 6-OHDA) lesion, medium dose (16 μg 6-OHDA) lesion, high dose (20 μg 6-OHDA) lesion. Bars represent mean ± S.E.M of net contralateral rotation for 10 minutes (n=5-6). There was a significant increase in the net contralateral rotations in all lesioned groups as compared to the sham group. **P<0.01 versus sham group (Newman-Keuls test) B) Apomorphine-induced rotational behaviour in animals lesioned in medial forebrain bundle fibers with 6-hydroxydopamine. Bars represent mean ± S.E.M of net contralateral rotation for 10 minutes (n=7-14). There was a significant increase in the net contralateral rotations in the lesioned group as compared to the sham group. ***p<0.0001 versus sham group (Unpaired student's test). Groups: Sham and lesions.

A)

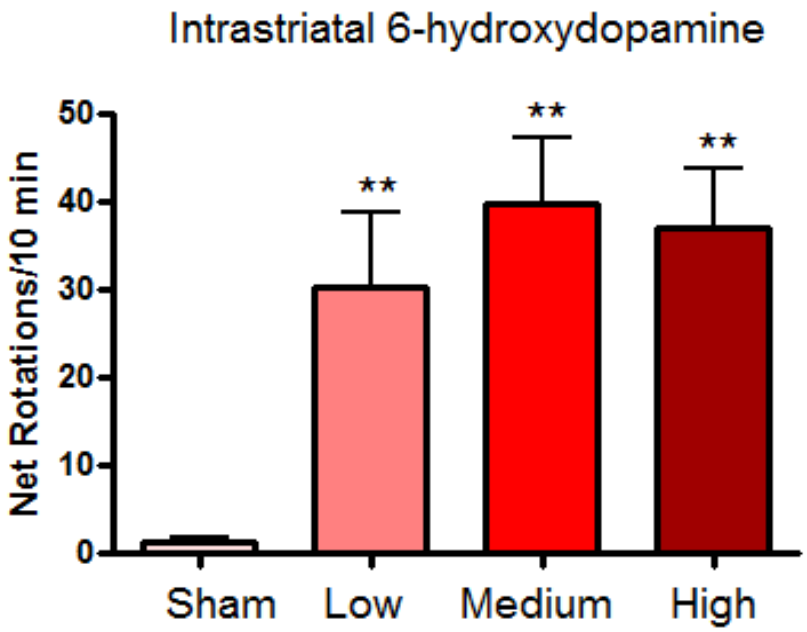
Intrastriatal 6-hydroxydopamine
Net Rotations/10 min
50
40
30
20
10
0
**
**
**
Sham
Low
Medium
High

B)

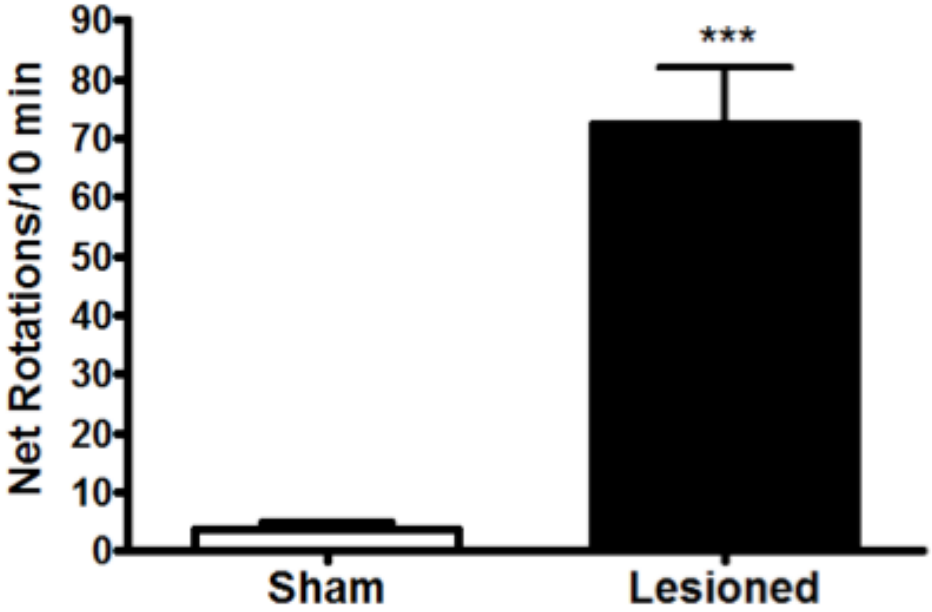
Net Rotations/10 min
90
80
70
60
50
40
30
20
10
0
***
Sham
Lesioned

Figure 4. TH immunoreactivity validation of the dopamine neurodegeneration induced by 6-hydroxydopamine in striatum. Left (a) and right (b) striatal tissue in 5x magnification, scale bar = 500μm and left (c) and right (d) striatal tissue in 63x magnification, scale bar = 50μm of the A) Sham animals, B) lesioned animals with 8.75 μg of 6-OHDA, C) lesioned animals with 16 μg of 6-OHDA and D) lesioned animals with 20 μg of 6-OHDA.

A) Sham

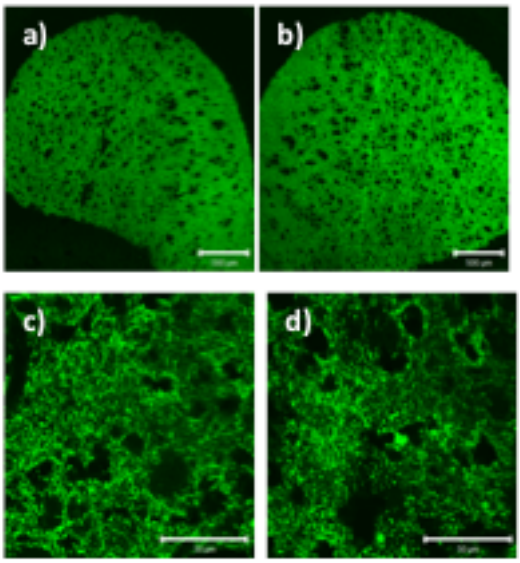

B) Low (8.75 µg) 6-OHDA

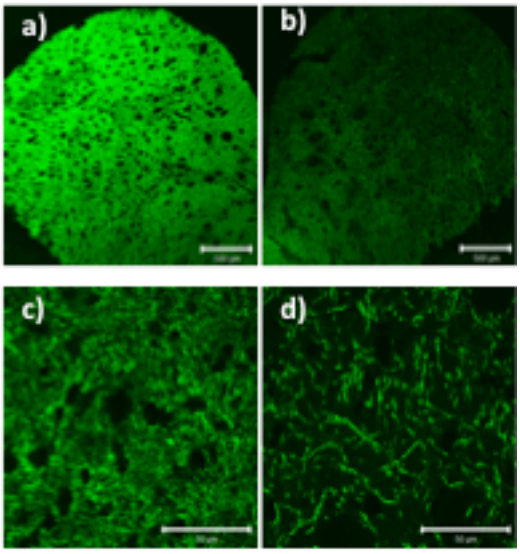

C) Medium (16 µg) 6-OHDA

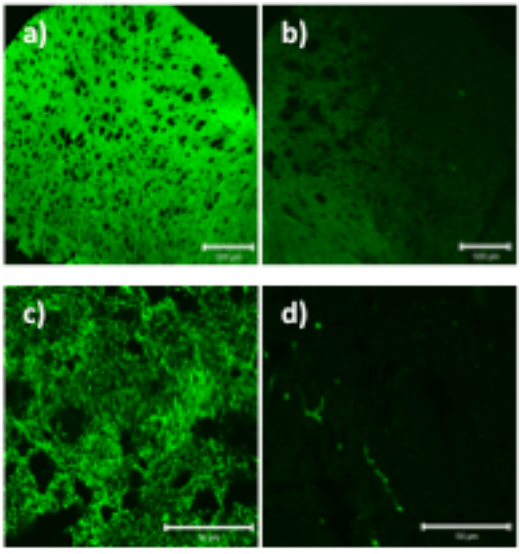

D) High (20 µg) 6-OHDA

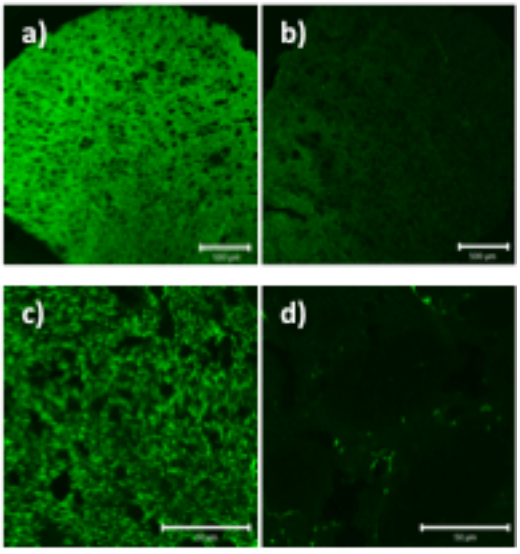

Figure 5. TH immunoreactivity validation of the dopamine neurodegeneration induced by 6-hydroxydopamine in substantia nigra. Left (a) and right (b) substantia nigral tissue in 5x magnification, scale bar = 500μm and left (c) and right (d) substantia nigral tissue in 20x magnification, scale bar = 100μm of the A) sham animals, B) lesioned animals with 8.75 μg of 6-OHDA, C) lesioned animals with 16 μg of 6-OHDA and D) lesioned animals with 20 μg of 6-OHDA.

A) Sham

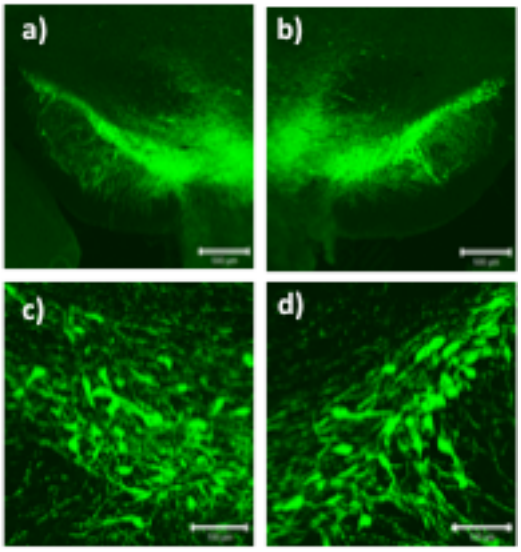

B) Low (8.75 µg) 6-OHDA

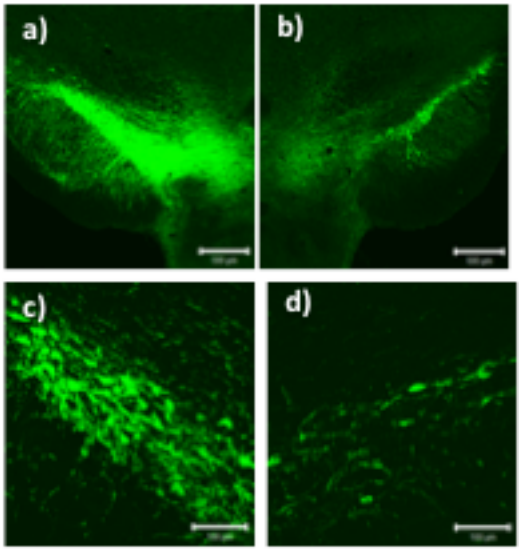

C) Medium (16 µg) 6-OHDA

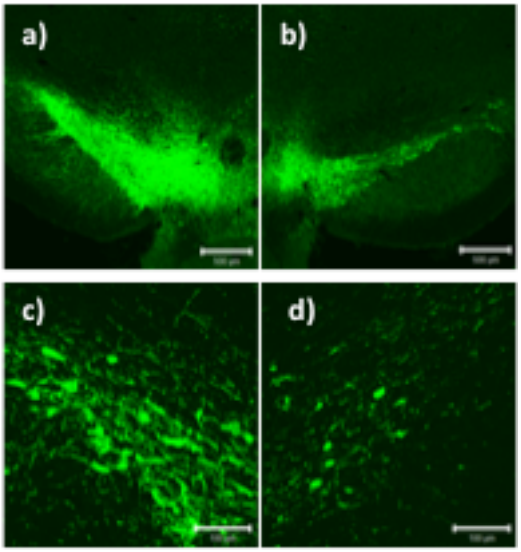

D) High (20 µg) 6-OHDA

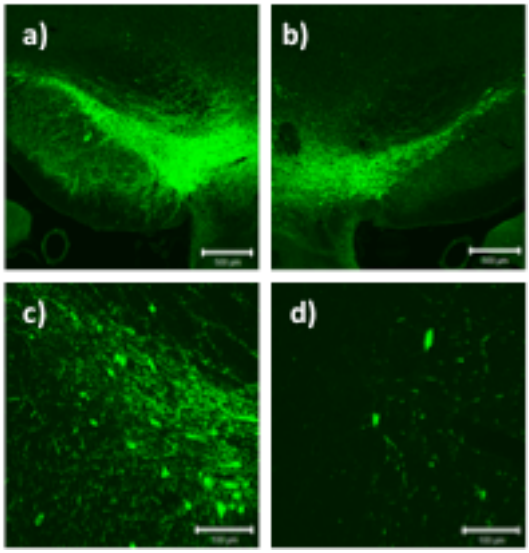

Figure 6. Tyrosine hydroxylase protein expression test on striatum from the ethanol and 2-methylbutane snap frozen brains. A) Striata dissected from 2-methylbutane snap frozen brains and 10 μg, 15 μg, and 25 μg of extracted protein loaded on gel. B) Striata dissected from ethanol frozen brains and 10 μg, 15 μg, and 25 μg of extracted protein loaded on gel.

A)

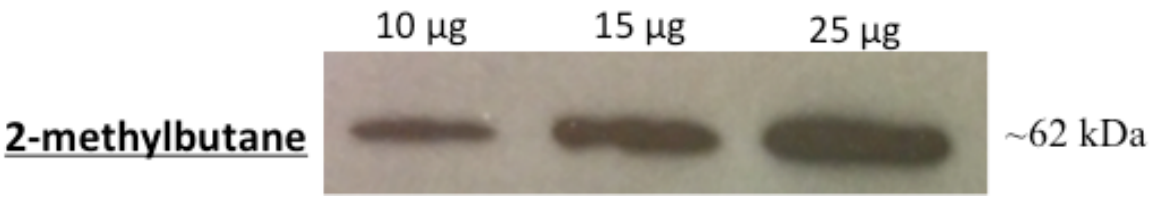
10 µg
15 µg
25 µg
2-methylbutane
~62 kDa

B)

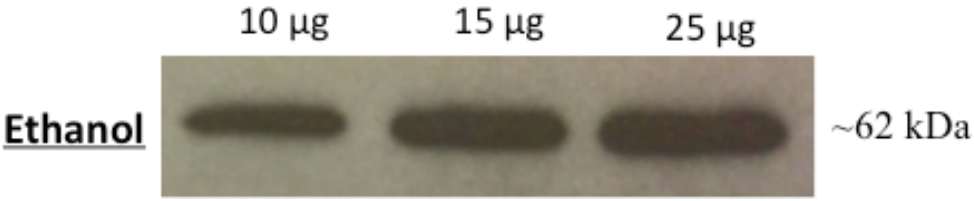
10 µg
15 µg
25 µg
Ethanol
~62 kDa

Figure 7. Western Blot protocol optimization for MT_1 protein expression. A. Protein concentration dependency was tested for MT_1 antibody using striatum and substantia nigra. Lanes (1-5): striatum 25 µg (1), 50 µg (2) and substantia nigra 25 µg (3), 50 µg (4), 75 µg (5). B. 24 hours MT_1 antibody incubation. C. 72 hours MT_1 antibody incubation MT_1 protein. Lanes (1-3): rat striatum (1), substantia nigra (2), and hypothalamus (3). D. MT_1 protein expression test using various lysis buffers on rat hypothalamus Lanes (1-3): original lysis buffer (1), lysis buffer 'a' (2), lysis buffer 'b' (3).

A)

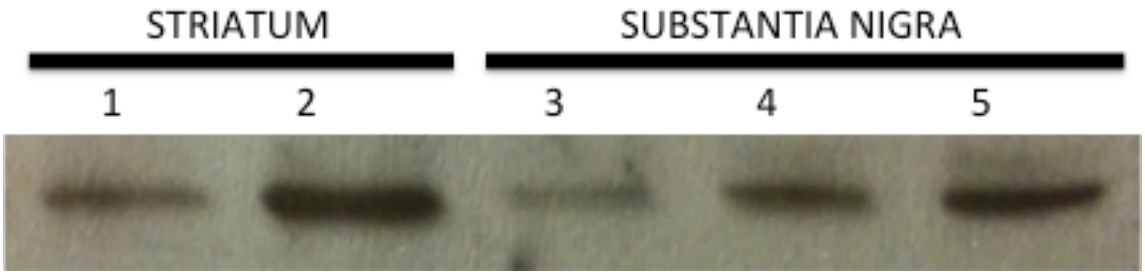
STRIATUM
SUBSTANTIA NIGRA
1
2
3
4
5

B)

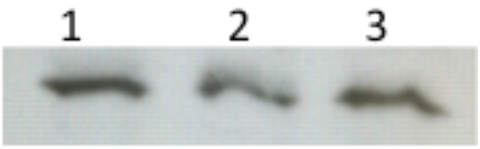
1
2
3

C)

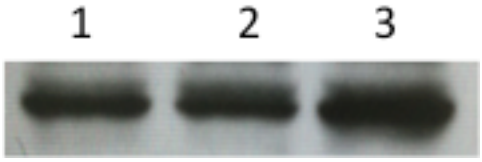
1
2
3

D)

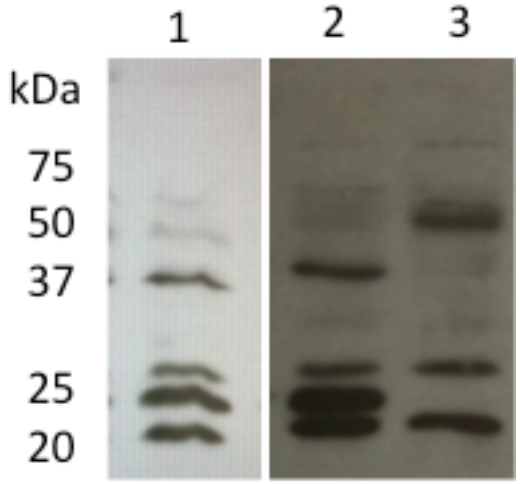
1
2
3
kDa
75
50
37
25
20

Figure 8. Validation of MT_1 primary antibody specificity *in vivo*. A) MT_1 antibody specificity test using blocking peptide as a negative control. MT_1 antibody (a) and pre-incubated MT_1 antibody with blocking peptide (b) were tested on hypothalamus (HTM) and substantia nigra (SN) tissues extracted with the original lysis buffer. B) Different lot numbered MT_1 antibody (a) and pre-incubated with blocking peptide (b) were tested on hypothalamus (HTM) and striatum (STR) in the same manner. C) MT_1 antibody specificity test using additional brain regions as a positive control. Lanes (1-5): hippocampus, cerebellum, striatum, substantia nigra, and hypothalamus.

A)

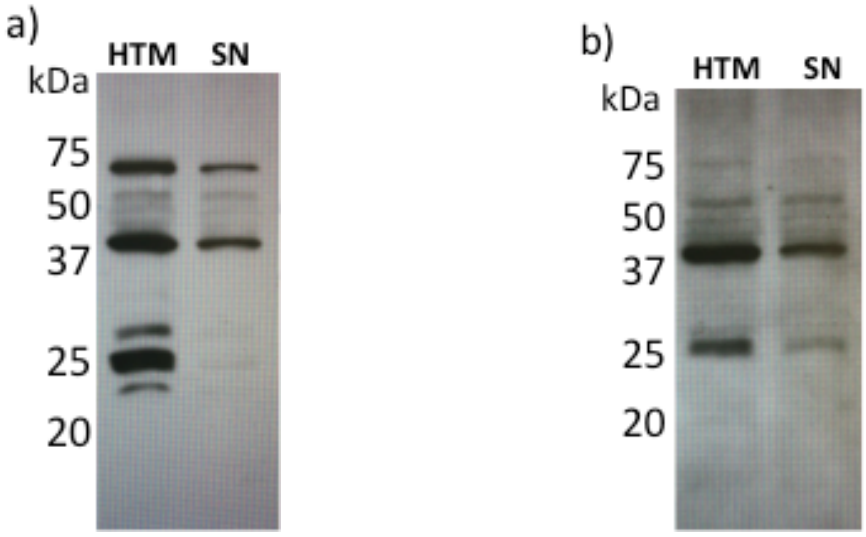
a)
HTM
SN
kDa
75
50
37
25
20
b)
HTM
SN
kDa
75
50
37
25
20

B)

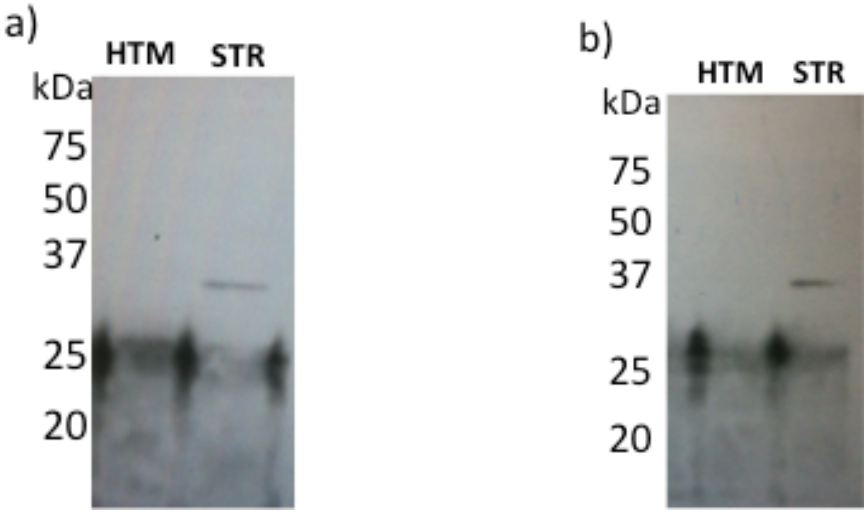
a)
HTM
STR
kDa
75
50
37
25
20
b)
HTM
STR
kDa
75
50
37
25
20

C)

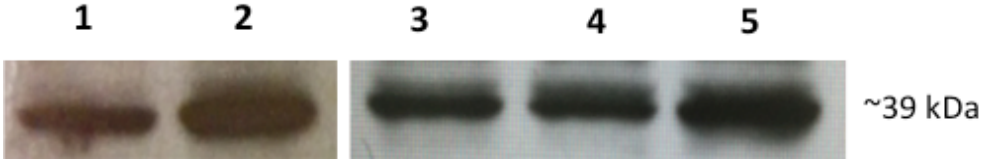
1
2
3
4
5
~39 kDa

Figure 9. Validation of MT_1 primary antibody specificity *in vitro*. A) MT_1 protein expression on Valproic acid (VPA) treated C17.2 cells. Lanes 1-4: control, 0.5mM VPA, 1mM VPA, 3mM VPA for 24 hours treatment. Lanes 5-7: control, 1mM VPA, 3mM VPA for 48 hours treatment. B) MT_1 protein expression on 24 hours VPA treated in C6 cells. Lanes 1-4: Control, 0.5mM VPA, 1mM VPA, 3mM VPA. C) HEK 293 cells (1) as a negative control, and rat hypothalamus (2) as a positive control was tested for antibody specificity validation.

A)

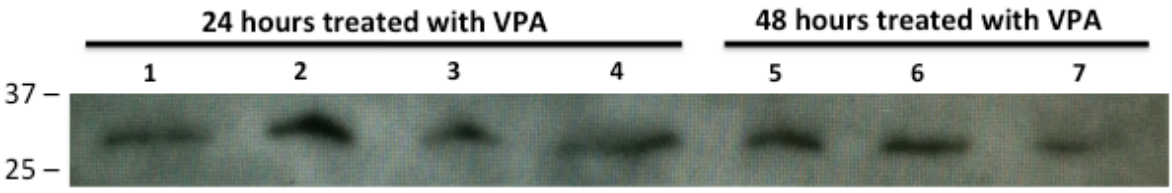
24 hours treated with VPA
48 hours treated with VPA
1
2
3
4
5
6
7
37 –
25 –

B)


1
2
3
4
37 –

C)

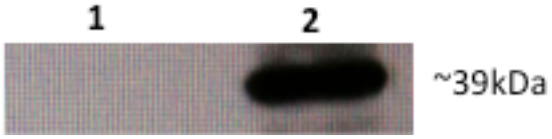
1
2
~39kDa

Figure 10. MT_1 protein expression level in striatum of intrastriatal 6-hydroxydopamine lesioned animals. Animals were lesioned in the right striatum with 8.75 μg (low), 16 μg (medium), and 20 μg (high) of 6-hydroxydopamine. A) Exposed film images of western blotting of MT_1 (~39 kDa) in the left and right striatum of sham and low, medium, and high 6-OHDA lesioned group. β-actin was used for the normalization of the data. B) Histogram bars represent the means ± S.E.M. for percentage of MT_1/ β-actin optical density (OD) ratio. White bars represent left striatum and black bars represent right striatum. No significance was observed between any groups.

A)

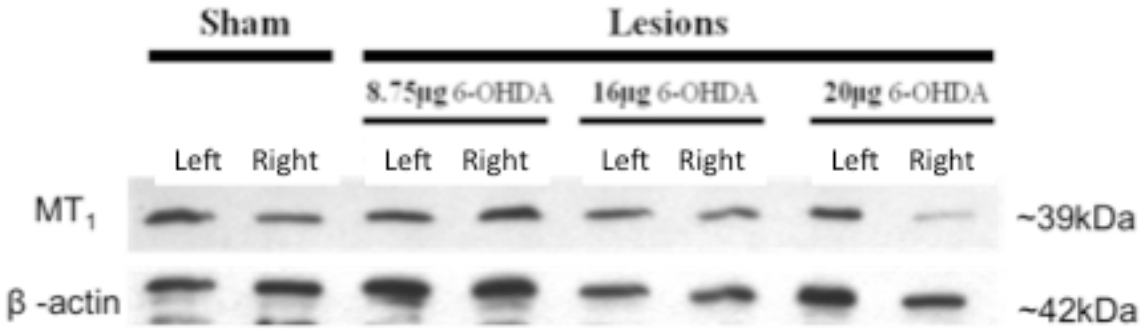
Sham
Lesions
8.75µg 6-OHDA
16µg 6-OHDA
20µg 6-OHDA
Left
Right
Left
Right
Left
Right
Left
Right
MT1
~39kDa
β -actin
~42kDa

B)

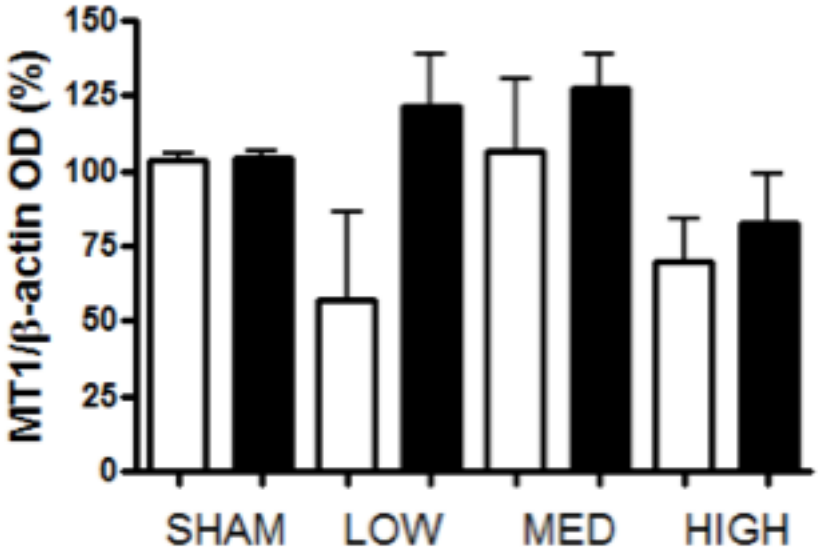
MT1/β-actin OD (%)
150
125
100
75
50
25
0
SHAM
LOW
MED
HIGH

Figure 11. MT_1 protein expression level in substantia nigra of intrastriatal 6-hydroxydopamine lesioned animals. Animals were lesioned in the right striatum with 8.75 μg (low), 16 μg (medium), and 20 μg (high) of 6-hydroxydopamine. A) Exposed film images of western blotting of MT_1 (~39 kDa) in the left and right substantia nigra of sham and low, medium, and high 6-OHDA lesioned group. β-actin was used for the normalization of the data. B) Histogram bars represent the means ± S.E.M. for percentage of MT_1/ β-actin optical density (OD) ratio. White bars represent left substantia nigra and black bars represent right substantia nigra. No significance was observed between any groups.

A)

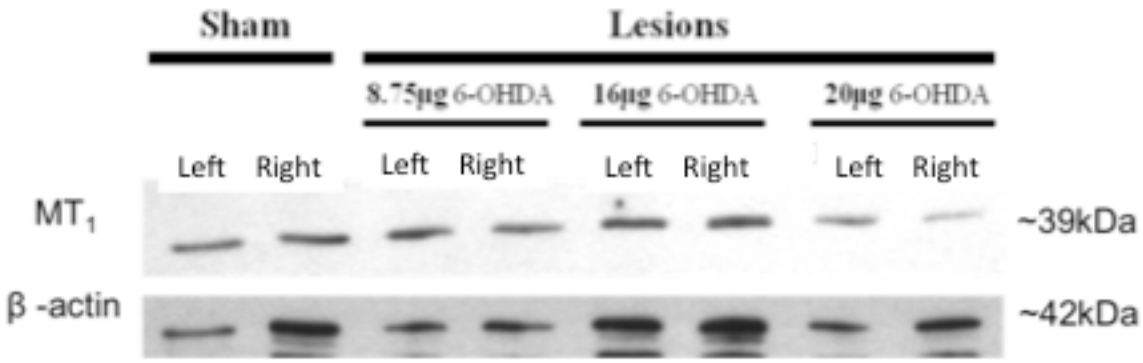
Sham
Lesions
8.75µg 6-OHDA
16µg 6-OHDA
20µg 6-OHDA
Left
Right
Left
Right
Left
Right
Left
Right
MT1
β -actin
~39kDa
~42kDa

B)

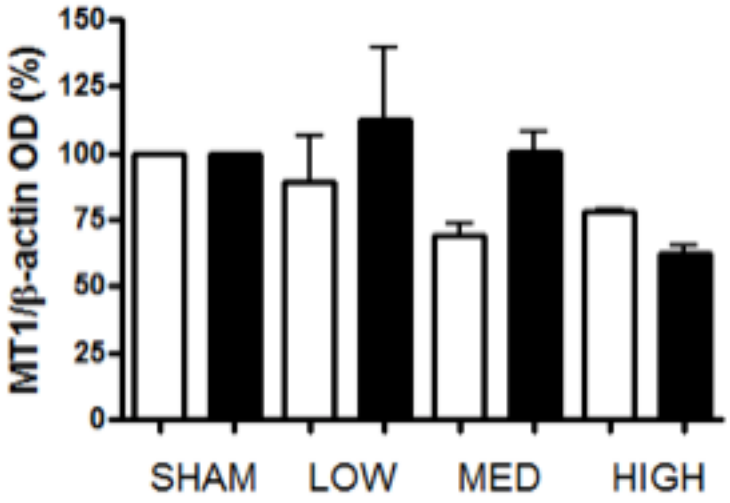
MT1/β-actin OD (%)
150
125
100
75
50
25
0
SHAM
LOW
MED
HIGH

Figure 12. MT_1 mRNA expression level in ventral midbrain of medial forebrain bundle lesioned animals. Animals were lesioned with 6-OHDA in the medial forebrain budle fibers. A) Gel images of MT_1 (441 bp) of the right (lesioned side) ventral midbrain and left (contralateral side, control) ventral midbrain after RT-PCR amplification. B) Histogram bars represent the means ± S.E.M. for percentage of MT_1/GAPDH optical density (OD) ratios of control (white bar) and lesioned (black bar) ventral midbrain. MT_1 mRNA expression in the lesioned ventral midbrain was significantly increased as compared to sham. **P<0.03 versus sham (Unpaired Student's test).

A)

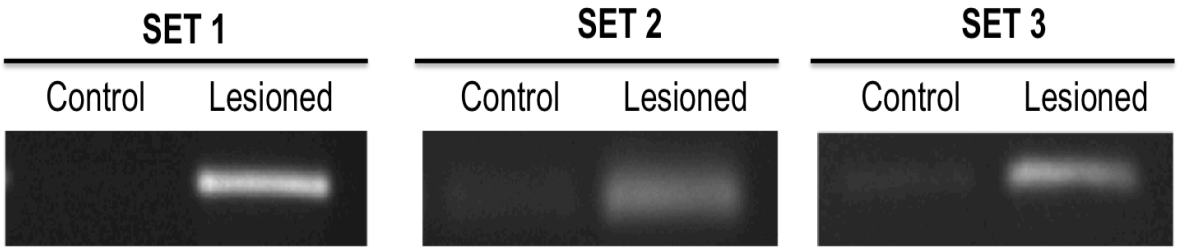
SET 1
Control
Lesioned
SET 2
Control
Lesioned
SET 3
Control
Lesioned

B)

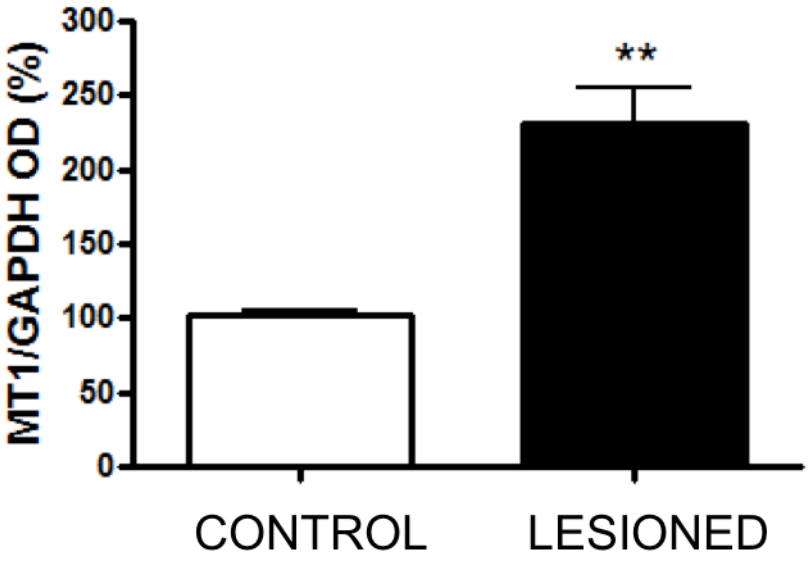
MT1/GAPDH OD (%)
300
250
200
150
100
50
0
**
CONTROL
LESIONED

3. Discussion

The first symptoms of Parkinson's disease do not appear until 50-70 % of the dopaminergic neurons have degenerated in the substantia nigra, and about 20 % of the dopaminergic neuron innervations remain in the striatum (Kirik et al., 1998; Mayo et al., 2005). 6-hydroxydopamine is neurotoxin which is widely used to generate the different stages of the Parkinson's disease animal model. It has been shown that the severity of dopaminergic neurodegeneration depends on the dose of 6-OHDA, the injection site and the spread of the toxin (ie, single or multiple injection sites) (Kirik et al., 1998). The unilateral intrastriatal single injection with 20 μg of 6-OHDA has been shown to destroy 60-70 % of TH immunoreactivity in the striatum and 0 – 25 % in the substantia nigra (Kirik et al., 1998). In previous studies, we have utilized a unilateral single injection site in the striatum with 8.75 μg and 16 μg of 6-OHDA with successful dopaminergic neurodegeneration (Sharma et al., 2006; Sharma et al., 2007). In this study, 8.75 μg, 16 μg, and 20 μg were used to generate different levels of severity in dopaminergic neurodegeneration, which can be implied as different stages of pre-symptomatic mild Parkinson's disease.

Furthermore, as Parkinson's disease advances, the loss of dopaminergic neurons progressively increases. At an advanced stage of Parkinson's disease, over 95% of dopamine terminal axons have been lost in the putamen and 60-80% of dopaminergic neurons have degenerated in the substantia nigra (Kirik et al., 1998). The unilateral two-site injections of 6-OHDA in the medial forebrain bundle shows a > 97% loss of

dopamine terminal axons in the striatum and a > 90% loss of dopaminergic neurons in the substantia nigra which is considered as a complete lesion of the nigrostriatal pathway (Kirik et al., 1998). In this study, the unilateral two-site injection of 6-OHDA in the medial forebrain bundle is also included to generate a terminal stage of the Parkinson's disease rat model.

Various behavioural tests can be used as tools to determine successful lesioning of the nigrostriatal pathway. In the present study, the apomorphine-induced rotational test and the forelimb asymmetry test have been included. Apomorphine is a non-selective dopamine agonist, which directly stimulates dopamine receptors. At 3 weeks post-surgery, injection of apomorphine caused a significant increase in net contralateral rotations ($p<0.01$) in both striatum (all doses of 6-OHDA) and medial forebrain bundle lesioned groups. The unilateral lesion either in striatum or medial forebrain bundle results in a one sided-depletion of dopaminergic neurons (Przedborski et al., 1995; Sauer & Oertel, 1994; Yuan et al., 2005). The depletion of dopaminergic neurons leads to a lack of dopamine availability and eventually results in upregulation of dopamine receptors at postsynaptic neurons in the striatum (Przedborski et al., 1995). Hence apomorphine injection leads to a functionally imbalanced stimulation between hemispheres, causing the animal to rotate in a contralateral direction away from to the lesioned side (Hudson et al., 1993). The significant increase in net contralateral rotations, observed in the present study, indicates that there was an upregulation of dopamine receptors and depletion of dopamine levels in the lesioned hemisphere, suggesting that a degeneration of

dopaminergic neurons was induced by 6-hydroxydopamine in both striatum and medial forebrain bundle lesioned animals.

Furthermore, the level of dopamine in striatum and substantia nigra correlates with apomorphine-induced rotational behaviour (Hudson et al., 1993). In the present study, the rotational behaviour in striatum lesioned animals showed between 30-40 net contralateral turns per 10 min, whereas medial forebrain bundle lesioned animals showed over 70 net contralateral turns per 10 min. The extensive rotational behaviour observed in the medial forebrain bundle lesioned animals indicates the presence of a more severe depletion of dopamine levels in striatum and substantia nigra induced by 6-OHDA, as compared to that in intrastriatal lesioned animals.

In order to assess possible motor deficit behaviours in the unilateral intrastriatal lesioned animals, the forelimb asymmetry test was utilized. This test examines the preferred side of the animal's forelimb usage by utilizing their natural instinct of exploring a novel environment by rearing and placing their forelimbs against the cylinder wall (Iancu et al., 2005). At 7 weeks post-surgery, a significant reduction of contralateral (left) forelimb usage was observed in the medium and the high doses of 6-OHDA lesioned groups as compared to the sham group. The reduction of contralateral forelimb use indicates successful depletion of dopaminergic neurons in the intrastriatal lesioned hemisphere induced by medium and high doses of 6-OHDA. Moreover, as mentioned above, the first symptoms of Parkinson's disease are seen when about 50-70% of

dopaminergic neurons have degenerated, and about 80% of the dopaminergic innervation to the striatum has been lost (Kirik et al., 1998; Mayo et al., 2005). The forelimb asymmetry test suggests that the medium and the high doses of 6-OHDA resulted in more severe dopaminergic neurodegeneration, possibly more than 50% of dopaminergic neurodegeneration, whereas the low dose of 6-OHDA lesions perhaps had less than 50% dopaminergic neurodegeneration, thus generating different level of mild Parkinson's disease animal model.

In addition to behavioural tests, immunoreactivity of tyrosine hydroxylase, a rate-limiting enzyme for dopamine synthesis, was also used to assess dopaminergic neurodegeneration induced by unilateral intrastriatal 6-OHDA lesions. At 8 weeks post-surgery, all lesioned groups showed a visible reduction in TH immunoreactivity on the lesioned side of the striatum and substantia nigra, as compared to the sham group. There were no changes in TH immunoreactivity in the contralateral striatum or substantia nigra of any groups. These results suggest a reduction in dopamine levels in the nigrostriatal pathway, which further suggests successful unilateral destruction of dopaminergic neurons induced by 6-OHDA. Furthermore, the level of TH immunoreactivity in the lesioned striatum was visibly lower in the medium and the high doses of 6-OHDA lesioned groups than in the low dose of 6-OHDA lesioned group. This indicates that the medium and the high doses of 6-OHDA resulted in a higher depletion of dopamine levels in the lesioned striatum than the low dose of 6-OHDA, which is consistent with the results of the forelimb asymmetry test.

Behavioural assessments, as well as changes in TH immunoreactivity showed a loss of phenotypic characteristics of dopaminergic activity in the nigrostriatal pathway, which suggests a loss of dopaminergic neurons in substantia nigra. Sauer and Oertel (1994) showed that intrastriatal 6-OHDA lesions resulted in a loss of TH immunoreactivity as observed in the present study, and a progressive loss of FluoroGold labeled nigra cells. Also, Yuan et al (2005) showed a positive correlation between the number of cells estimated by TH immunoreactivity and Nissl-positive cells in substantia nigra of the intrastriatal and medial forebrain bundle lesion models. Moreover, many studies have shown that animals with significant increase in apomorphine induced rotational behaviour also showed a loss of dopamine contents, dopamine uptake sites and TH immunoreactivity in nigrostriatal pathway, following 6-OHDA lesions in either striatum or medial forebrain bundle (Hudson et al., 1993; Kirik et al., 1998; Przedborski et al., 1995). Therefore, our behavioural tests and TH immunoreactivity are good indicators of 6-OHDA induced dopaminergic neurodegeneration. In future studies, a neuronal marker, such as Nissl staining would be helpful to validate the degeneration of neurons induced by 6-OHDA.

The key objective for this study was to evaluate melatonin receptor expression following 6-OHDA lesions. Therefore, after confirming lesion-induced degeneration of the dopaminergic pathway, assessment of the mRNA and protein levels of melatonin receptors in the nigrostriatal pathway were performed. The initial plan to assess the

mRNA level of MT_1 and MT_2 receptors in striatum, hippocampus, and substantia nigra by *in situ* hybridization was not successful. Therefore, it was decided to proceed with western blot and RT-PCR for the assessment of melatonin receptor levels in the nigrostriatal pathway, following the 6-OHDA lesions.

Prior to assessing protein level of melatonin receptors by western blot, optimization of the protocol was required. The snap-freezing method of preserving tissues was typically carried out with 2-methylbutane for *in situ* hybridization. However, since the harvested brains were snap frozen in ethanol instead of 2-methylbutane, we ran a quick test to see whether the protein is preserved in the ethanol frozen brains. Two non-lesioned practice rats were sacrificed and harvested brains were snap frozen either by ethanol or 2-methylbutane. The protein was extracted from the dissected striatum from both brains and tested for tyrosine hydroxylase, which is highly expressed in this region. Both 2-methylbutane and ethanol snap frozen tissues allowed detection of TH protein, indicating that both methods can be used for protein analysis by western blotting. In addition to TH antibody, MT_1 and MT_2 antibodies were also tested on the striatum, substantia nigra, hippocampus and hypothalamus from the ethanol frozen brain. However, the MT_2 antibody failed to show any reactivity on the membrane. A second MT_2 antibody, which binds to a different epitope, was also tested, but no bands were detected. Because currently available MT_2 antibodies are ineffective, subsequent protein analysis was focused on MT_1 receptor.

In order to evaluate the optimal protein amounts to be loaded on the SDS-PAGE gel for MT_1 antibody, different amounts of total protein from striatum (25 μg, 50 μg) and substantia nigra (20 μg, 50 μg, and 75 μg) were tested. After the exposure on to the film, the anticipated MT_1 protein band, which is around 39 kDa, was detected in all amounts of the striatum and the substantia nigra tested. 75 μg of protein gave oversaturated bands, indicating that it is not an optimal protein amount to distinguish any possible differences between samples. The best result was obtained with 25-50 μg of striatum and substantia nigra, so 50 μg of protein was used to pursue further analysis.

Subsequently, the optimal MT_1 primary antibody incubation time was evaluated. Two western blot membranes, which contain striatum, substantia nigra and hypothalamus protein samples, were incubated with MT_1 primary antibody either for 24 hours or 72 hours. 24-hours primary antibody incubation was sufficient to detect the anticipated MT_1 protein bands, whereas 72-hours incubation showed oversaturated bands thus 24 hours incubation was chosen for the future analysis.

Three different lysis buffers were used to examine the quality of the protein extraction and possibly eliminate non-specific bindings. Hypothalamus was used for this test since it is known to express high levels of MT_1 receptors. Lysis buffer ‘a’ was made as per previous studies where verified MT_1 antibody was utilized (Castro et al., 2005). Lysis buffer ‘b’ was obtained from a published paper, which used the same MT_1 antibody from Abbiotec™ as in the present study (Wang et al., 2012). Interestingly, the standard

and 'a' lysis buffer revealed similar results, which showed anticipated MT_1 and non-specific bands. However, lysis buffer 'b' eliminated the anticipated MT_1 bands and showed non-specific bands. Lysis buffer 'b' used 100 fold lower amounts of detergent, which may have been insufficient for effective cytosolic protein extraction. Therefore, for further analysis, standard lysis buffer was utilized. Lastly, the primary antibody was omitted in the protocol to examine possible non-specific binding of the secondary antibody. No bands were detected (blots not shown) when the primary antibody was omitted. Hence, the non-specific bands were detected by the polyclonal primary antibody.

The MT_1 antibody used in this present study has not been verified for the specific reactivity to MT_1 receptors. To validate the specificity of the MT_1 antibody, various tests were performed. First, a blocking peptide was utilized as a negative control on rat hypothalamus and substantia nigra. The blocking peptide should pre-absorb the MT_1 antibody, which disables the binding to the MT_1 antigen. However, the anticipated MT_1 band (~39 kDa) still appeared on the blocked antibody blot, indicating possibilities of a false positive result or ineffective blocking peptide.

Additional brain regions, which are known to express MT_1 receptors, such as cerebellum (Al-Ghoul et al., 1998), hippocampus (Savaskan et al., 2002), and hypothalamus (Morgan et al., 1994) were also included for the MT_1 antibody specificity test. The anticipated MT_1 bands as well as non-specific bands were observed in all additional brain regions. Studies have reported that the MT_1 receptor is more enriched in

hypothalamus, which contains the suprachiasmatic nucleus and in the cerebellum, than in the hippocampus (Mazzucchelli et al., 1996). The MT_1 antibody used in this study had detected the highest protein expression level in hypothalamus and cerebellum, which is consistent with published results.

Further specificity validation of the MT_1 antibody was performed *in vitro*. Niles et al (2004) had shown that C17.2 mouse neural stem cells (NSCs) express MT_1 receptor with a validated MT_1 antibody from CIDTech. Interestingly, MT_1 protein obtained from the short-term cultured C17.2 NSCs is detected at a lower molecular weight (~30 kDa) due to the immaturity of the protein, which hasn't gone through posttranslational modifications and translocation to the plasma membrane (Niles et al., 2004). When the MT_1 antibody from Abbiotec™ was tested on C17.2 NSCs, a single band around 30 kDa was observed as reported previously. This result further supports the specificity of the MT_1 antibody used in this present study.

In previous studies, MT_1 receptor protein expression was detected with a (no longer available) validated antibody (CIDTech) in C6 cells (Castro et al., 2005). It was reported that MT_1 protein expression was upregulated in a concentration-dependent manner by VPA, with the highest MT_1 expression level observed at 1mM VPA treatment (Castro et al., 2005). The MT_1 antibody used in this study revealed the same increasing trend at the anticipated MT_1 bands (around 39 kDa), supporting the specificity of the

antibody. However, the non-specific bands were again observed in C6 rat glioma cells as seen in rat tissues.

As an *in vitro* negative control, human embryonic kidney (HEK) 293 cells without any transfection were utilized to test MT_1 antibody specificity. The MT_1 antibody used in this study did not detect the MT_1 band or the non-specific bands seen with other tissues. Based on these findings, it appears that the MT_1 antibody is specifically reacting to the antigen of the MT_1 receptor, and it can be used to detect receptor protein expression.

Subsequent to western optimization and partial validation of the MT_1 antibody specificity, MT_1 receptor expression levels in striatum and substantia nigra of the unilateral intrastriatal 6-OHDA lesioned animals were examined. The tissues were collected from each cerebral hemisphere of all groups, which were sacrificed after 8 weeks post-surgery. There were no significant changes of MT_1 protein expression levels in the lesioned and the intact striatum between the sham group and 6-OHDA intrastriatal lesioned groups. Moreover, no significant differences of MT_1 protein expression levels were observed in the lesioned and the intact substantia nigra between the sham group and 6-OHDA intrastriatal lesioned groups. Therefore, mild dopaminergic neurodegeneration in the nigrostriatal pathway does not alter MT_1 receptor level in striatum and substantia nigra. Lin et al. (2013) reported that the extracellular level of melatonin was increased in both lesioned and intact striatum of the complete lesioned hemiparkinsonian rat (induced by 6-OHDA, which involves over 85% of dopaminergic neurodegeneration in

nigrostriatal pathway). Interestingly, the increase in extracellular melatonin levels in the lesioned striatum was not observed at 3 weeks post-lesion, but was observed after 4 weeks, at which time there was an 85% reduction of dopamine levels in striatum (Lin et al., 2013). In subsequent weeks post-lesion, there was a progressive loss of dopamine levels in striatum (Lin et al., 2013). It has been reported that medial forebrain bundle 6-OHDA lesioned animals showed 78% of cell loss in the substantia nigra at 3 weeks post-lesion, and showed further loss to 88% at 5 weeks (Yuan et al., 2005). Therefore, less than 85% reduction of dopamine level in striatum does not elevate the endogenous melatonin level in striatum (Lin et al., 2013). Similar mild Parkinson's disease models as used in the present study, have shown a reduction of 60-70% of dopamine level in striatum (Kirik et al., 1998). Therefore, the endogenous melatonin level in striatum is not likely to change in the mild Parkinson's disease model. As observed in the present study, the absence of significant differences of MT_1 protein expression in striatum and substantia nigra, between control and lesioned groups might be due to less severe dopaminergic neurodegeneration, following intrastriatal lesioning. However, it would be worthwhile to replicate westerns of MT_1 protein levels in the lesioned striatum and substantia nigra, using a definitively validated antibody.

In this study, melatonin receptor expression was also examined in the advanced stage of the hemiparkinsonian rat model, which was created by 6-OHDA lesions in the medial forebrain bundle. At four weeks post-surgery, MT_1 mRNA expression levels in the lesioned (right) ventral midbrains of the lesioned group was significantly ($p<0.03$)

upregulated as compared to the contralateral ventral midbrains of the same animals. As mentioned above, the severe depletion of dopaminergic neurons in the nigrostriatal pathway showed an increase in the extracellular melatonin level in striatum (Lin et al., 2013). There have been reports of an increase in serum melatonin in hemiparkinsonian rats, as well as in patients with Parkinson's disease (Catala et al., 1997; Lin et al., 2014). Along with the elevated melatonin level in striatum (Lin et al., 2013), the increase in MT_1 receptor expression in the lesioned ventral midbrain observed in the present study may be a neuroprotective response against dopaminergic neurodegeneration, since the activation of this receptor can trigger various downstream pathways, which promote cell protection and survival (Koh, 2008; Luchetti et al., 2010), as well as increasing the expression of antioxidative enzymes (Mayo et al., 2002; Rodriguez et al., 2004). Many studies have shown the neuroprotective and antioxidative effects of the melatonergic system against dopaminergic neurodegeneration in the nigrostriatal pathway. Chronic treatment with a physiological dose of melatonin is neuroprotective as indicated by preservation of tyrosine hydroxylase immunoreactivity in the striatum of the intrastriatal 6-OHDA lesioned rat (Sharma et al., 2006). A higher (pharmacological) dose of melatonin in 6-OHDA Parkinson's disease models acted as a potent antioxidant, hence preventing oxidative damage and apoptosis (Joo et al., 1998; Mayo et al., 2005). Moreover, transplantation of MT_1 receptor-expressing mouse neural stem cells (C17.2), together with melatonin treatment, was shown to preserve dopaminergic integrity in 6-OHDA lesioned animals (Sharma et al., 2007). Therefore, we speculate that severe destruction of the dopaminergic system in the nigrostriatal pathway leads to an increase in endogenous

melatonergic signaling as a compensatory phenomenon to protect residual dopaminergic neurons. Similarly, in Alzheimer disease, which is another neurodegenerative disorder, upregulation of MT_1 expression level was observed in human hippocampus (Savaskan et al., 2002), supporting the possibility of compensatory neuroprotective mechanism exerted via the MT_1 receptor. However studies have reported that the progression of other neurodegenerative diseases is associated with loss of the MT_1 receptor. Zhang et al (2013) has reported that the progression of amyotrophic lateral sclerosis was linked with losses of melatonin and MT_1 receptor in the mouse spinal cord. Also, as Huntington disease progresses, MT_1 receptor levels were depleted in mouse brain and human striatum (Wang et al., 2011). These studies suggest a possible relationship between lack of compensatory neuroprotective responses exerted by MT_1 receptor and the progression of neurodegenerative diseases. In this present study, the upregulation of MT_1 receptor mRNA level was only observed in the terminal stage of Parkinson's disease model, and no alteration of MT_1 protein level was observed in the mild stage of Parkinson's disease model. This suggests that the possible compensatory neuroprotective response of MT_1 receptor is only triggered in the terminal stage of the Parkinson's disease, which may not recover degenerated dopaminergic neurons but perhaps slows down the further progression of dopaminergic neurodegeneration in the nigrostriatal pathway. In contrast to the present observation, a single report showed a downregulation of the MT_1 receptor in the post-mortem substantia nigra of patients with Parkinson's disease (Adi et al., 2010). The reason for this discrepancy may be due to various factors including species, sex, age, time of death, and severity of dopaminergic neurodegeneration. Further studies of

melatonin MT_1 and MT_2 mRNA and protein expression in striatum and ventral midbrain in relation to progression of dopaminergic neurodegeneration, should be performed to confirm the neuroprotective interaction between the melatonergic and dopaminergic systems, and possibly elucidate the mechanism of possible compensatory neuroprotective response exerted by MT_1 in Parkinson's disease.

5. Bibliography

Adi, N., Mash, D. C., Ali, Y., Singer, C., Shehadeh, L., & Papapetropoulos, S. (2010). Melatonin MT1 and MT2 receptor expression in parkinson's disease. *Medical Science Monitor : International Medical Journal of Experimental and Clinical Research, 16*(2), BR61-7.

Al-Ghoul, W. M., Herman, M. D., & Dubocovich, M. L. (1998). Melatonin receptor subtype expression in human cerebellum. *Neuroreport, 9*(18), 4063-4068.

Armstrong, K. J., & Niles, L. P. (2002). Induction of GDNF mRNA expression by melatonin in rat C6 glioma cells. *Neuroreport, 13*(4), 473-475.

Bahna, S. G., Sathiyapalan, A., Foster, J. A., & Niles, L. P. (2014). Regional upregulation of hippocampal melatonin MT2 receptors by valproic acid: Therapeutic implications for alzheimer's disease. *Neuroscience Letters, 576*, 84-87.

Berson, D. M., Dunn, F. A., & Takao, M. (2002). Phototransduction by retinal ganglion cells that set the circadian clock. *Science (New York, N.Y.), 295*(5557), 1070-1073.

Blandini, F., Balestra, B., Levandis, G., Cervio, M., Greco, R., Tassorelli, C., et al. (2009). Functional and neurochemical changes of the gastrointestinal tract in a rodent model of parkinson's disease. *Neuroscience Letters, 467*(3), 203-207.

Bove, J., Prou, D., Perier, C., & Przedborski, S. (2005). Toxin-induced models of parkinson's disease. *NeuroRx : The Journal of the American Society for Experimental NeuroTherapeutics, 2*(3), 484-494.

Castro, L. M., Gallant, M., & Niles, L. P. (2005). Novel targets for valproic acid: Up-regulation of melatonin receptors and neurotrophic factors in C6 glioma cells. *Journal of Neurochemistry, 95*(5), 1227-1236.

Catala, M. D., Canete-Nicolas, C., Iradi, A., Tarazona, P. J., Tormos, J. M., & Pascual-Leone, A. (1997). Melatonin levels in parkinson's disease: Drug therapy versus electrical stimulation of the internal globus pallidus. *Experimental Gerontology, 32*(4-5), 553-558.

Claustrat, B., Brun, J., & Chazot, G. (2005). The basic physiology and pathophysiology of melatonin. *Sleep Medicine Reviews, 9*(1), 11-24.

Doolen, S., Krause, D. N., Dubocovich, M. L., & Duckles, S. P. (1998). Melatonin mediates two distinct responses in vascular smooth muscle. *European Journal of Pharmacology, 345*(1), 67-69.

Drazen, D. L., & Nelson, R. J. (2001). Melatonin receptor subtype MT2 (mel 1b) and not mt1 (mel 1a) is associated with melatonin-induced enhancement of cell-mediated and humoral immunity. *Neuroendocrinology, 74*(3), 178-184.

Dubocovich, M. L. (1983). Melatonin is a potent modulator of dopamine release in the retina. *Nature, 306*(5945), 782-784.

Dubocovich, M. L., Delagrange, P., Krause, D. N., Sugden, D., Cardinali, D. P., & Olcese, J. (2010). International union of basic and clinical pharmacology. LXXV. nomenclature, classification, and pharmacology of G protein-coupled melatonin receptors. *Pharmacological Reviews, 62*(3), 343-380.

Dubocovich, M. L., & Markowska, M. (2005). Functional MT1 and MT2 melatonin receptors in mammals. *Endocrine, 27*(2), 101-110.

Dubocovich, M. L., Rivera-Bermudez, M. A., Gerdin, M. J., & Masana, M. I. (2003). Molecular pharmacology, regulation and function of mammalian melatonin receptors. *Frontiers in Bioscience : A Journal and Virtual Library, 8*, d1093-108.

Ferguson, S. S. (2001). Evolving concepts in G protein-coupled receptor endocytosis: The role in receptor desensitization and signaling. *Pharmacological Reviews, 53*(1), 1-24.

Ganguly, S., Coon, S. L., & Klein, D. C. (2002). Control of melatonin synthesis in the mammalian pineal gland: The critical role of serotonin acetylation. *Cell and Tissue Research, 309*(1), 127-137.

Gauer, F., Masson-Pevet, M., Saboureau, M., George, D., & Pevet, P. (1993). Differential seasonal regulation of melatonin receptor density in the pars tuberalis and the

suprachiasmatic nuclei: A study in the hedgehog (erinaceus europaeus, L.). *Journal of Neuroendocrinology, 5*(6), 685-690.

Gerdin, M. J., Masana, M. I., Ren, D., Miller, R. J., & Dubocovich, M. L. (2003). Short-term exposure to melatonin differentially affects the functional sensitivity and trafficking of the hMT1 and hMT2 melatonin receptors. *The Journal of Pharmacology and Experimental Therapeutics, 304*(3), 931-939.

Gillette, M. U., & Mitchell, J. W. (2002). Signaling in the suprachiasmatic nucleus: Selectively responsive and integrative. *Cell and Tissue Research, 309*(1), 99-107.

Gomez-Lazaro, M., Galindo, M. F., Concannon, C. G., Segura, M. F., Fernandez-Gomez, F. J., Llecha, N., et al. (2008). 6-hydroxydopamine activates the mitochondrial apoptosis pathway through p38 MAPK-mediated, p53-independent activation of bax and PUMA. *Journal of Neurochemistry, 104*(6), 1599-1612.

Hamdi, A. (1998). Melatonin administration increases the affinity of D2 dopamine receptors in the rat striatum. *Life Sciences, 63*(23), 2115-2120.

Hankins, M. W., Peirson, S. N., & Foster, R. G. (2008). Melanopsin: An exciting photopigment. *Trends in Neurosciences, 31*(1), 27-36.

Hardeland, R. (2008). Melatonin, hormone of darkness and more: Occurrence, control mechanisms, actions and bioactive metabolites. *Cellular and Molecular Life Sciences : CMLS, 65*(13), 2001-2018.

Hudson, J. L., van Horne, C. G., Stromberg, I., Brock, S., Clayton, J., Masserano, J., et al. (1993). Correlation of apomorphine- and amphetamine-induced turning with nigrostriatal dopamine content in unilateral 6-hydroxydopamine lesioned rats. *Brain Research, 626*(1-2), 167-174.

Hunt, A. E., Al-Ghoul, W. M., Gillette, M. U., & Dubocovich, M. L. (2001). Activation of MT(2) melatonin receptors in rat suprachiasmatic nucleus phase advances the circadian clock. *American Journal of Physiology.Cell Physiology, 280*(1), C110-8.

Iancu, R., Mohapel, P., Brundin, P., & Paul, G. (2005). Behavioral characterization of a unilateral 6-OHDA-lesion model of parkinson's disease in mice. *Behavioural Brain Research, 162*(1), 1-10.

Jiang, Z. G., Nelson, C. S., & Allen, C. N. (1995). Melatonin activates an outward current and inhibits ih in rat suprachiasmatic nucleus neurons. *Brain Research, 687*(1-2), 125-132.

Jimenez-Jorge, S., Jimenez-Caliani, A. J., Guerrero, J. M., Naranjo, M. C., Lardone, P. J., Carrillo-Vico, A., et al. (2005). Melatonin synthesis and melatonin-membrane receptor (MT1) expression during rat thymus development: Role of the pineal gland. *Journal of Pineal Research, 39*(1), 77-83.

Joo, W. S., Jin, B. K., Park, C. W., Maeng, S. H., & Kim, Y. S. (1998). Melatonin increases striatal dopaminergic function in 6-OHDA-lesioned rats. *Neuroreport, 9*(18), 4123-4126.

Karasek, M. (2004). Melatonin, human aging, and age-related diseases. *Experimental Gerontology, 39*(11-12), 1723-1729.

Kirik, D., Rosenblad, C., & Bjorklund, A. (1998). Characterization of behavioral and neurodegenerative changes following partial lesions of the nigrostriatal dopamine system induced by intrastriatal 6-hydroxydopamine in the rat. *Experimental Neurology, 152*(2), 259-277.

Koh, P. O. (2008). Melatonin prevents the injury-induced decline of akt/forkhead transcription factors phosphorylation. *Journal of Pineal Research, 45*(2), 199-203.

Lin, L., Du, Y., Yuan, S., Shen, J., Lin, X., & Zheng, Z. (2014). Serum melatonin is an alternative index of parkinson's disease severity. *Brain Research, 1547*, 43-48.

Lin, L., Meng, T., Liu, T., & Zheng, Z. (2013). Increased melatonin may play dual roles in the striata of a 6-hydroxydopamine model of parkinson's disease. *Life Sciences, 92*(4-5), 311-316.

Liu, C., Weaver, D. R., Jin, X., Shearman, L. P., Pieschl, R. L., Gribkoff, V. K., et al. (1997). Molecular dissection of two distinct actions of melatonin on the suprachiasmatic circadian clock. *Neuron, 19*(1), 91-102.

Luchetti, F., Canonico, B., Betti, M., Arcangeletti, M., Pilolli, F., Piroddi, M., et al. (2010). Melatonin signaling and cell protection function. *FASEB Journal : Official*

Publication of the Federation of American Societies for Experimental Biology, 24(10), 3603-3624.

MacKenzie, R. S., Melan, M. A., Passey, D. K., & Witt-Enderby, P. A. (2002). Dual coupling of MT(1) and MT(2) melatonin receptors to cyclic AMP and phosphoinositide signal transduction cascades and their regulation following melatonin exposure. *Biochemical Pharmacology, 63*(4), 587-595.

Mayo, J. C., Sainz, R. M., Antoli, I., Herrera, F., Martin, V., & Rodriguez, C. (2002). Melatonin regulation of antioxidant enzyme gene expression. *Cellular and Molecular Life Sciences : CMLS, 59*(10), 1706-1713.

Mayo, J. C., Sainz, R. M., Tan, D. X., Antolin, I., Rodriguez, C., & Reiter, R. J. (2005). Melatonin and parkinson's disease. *Endocrine, 27*(2), 169-178.

Mazzucchelli, C., Pannacci, M., Nonno, R., Lucini, V., Fraschini, F., & Stankov, B. M. (1996). The melatonin receptor in the human brain: Cloning experiments and distribution studies. *Brain Research.Molecular Brain Research, 39*(1-2), 117-126.

McArthur, A. J., Hunt, A. E., & Gillette, M. U. (1997). Melatonin action and signal transduction in the rat suprachiasmatic circadian clock: Activation of protein kinase C at dusk and dawn. *Endocrinology, 138*(2), 627-634.

McMillan, C. R., Sharma, R., Ottenhof, T., & Niles, L. P. (2007). Modulation of tyrosine hydroxylase expression by melatonin in human SH-SY5Y neuroblastoma cells. *Neuroscience Letters, 419*(3), 202-206.

Mishima, K., Okawa, M., Shimizu, T., & Hishikawa, Y. (2001). Diminished melatonin secretion in the elderly caused by insufficient environmental illumination. *The Journal of Clinical Endocrinology and Metabolism, 86*(1), 129-134.

Morgan, P. J., Barrett, P., Howell, H. E., & Helliwell, R. (1994). Melatonin receptors: Localization, molecular pharmacology and physiological significance. *Neurochemistry International, 24*(2), 101-146.

Moriya, T., Horie, N., Mitome, M., & Shinohara, K. (2007). Melatonin influences the proliferative and differentiative activity of neural stem cells. *Journal of Pineal Research, 42*(4), 411-418.

Niles, L. P., Armstrong, K. J., Rincon Castro, L. M., Dao, C. V., Sharma, R., McMillan, C. R., et al. (2004). Neural stem cells express melatonin receptors and neurotrophic factors: Colocalization of the MT1 receptor with neuronal and glial markers. *BMC Neuroscience, 5*, 41.

Nosjean, O., Ferro, M., Coge, F., Beauverger, P., Henlin, J. M., Lefoulon, F., et al. (2000). Identification of the melatonin-binding site MT3 as the quinone reductase 2. *The Journal of Biological Chemistry, 275*(40), 31311-31317.

Pandi-Perumal, S. R., Srinivasan, V., Maestroni, G. J., Cardinali, D. P., Poeggeler, B., & Hardeland, R. (2006). Melatonin: Nature's most versatile biological signal? *The FEBS Journal, 273*(13), 2813-2838.

Pandi-Perumal, S. R., Trakht, I., Srinivasan, V., Spence, D. W., Maestroni, G. J., Zisapel, N., et al. (2008). Physiological effects of melatonin: Role of melatonin receptors and signal transduction pathways. *Progress in Neurobiology, 85*(3), 335-353.

Petit, L., Lacroix, I., de Coppet, P., Strosberg, A. D., & Jockers, R. (1999). Differential signaling of human Mel1a and Mel1b melatonin receptors through the cyclic guanosine 3'-5'-monophosphate pathway. *Biochemical Pharmacology, 58*(4), 633-639.

Pongsa-Asawapaiboon, A., Asavaritikrai, P., Withyachumnarnkul, B., & Sumridthong, A. (1998). Melatonin increases nerve growth factor in mouse submandibular gland. *Journal of Pineal Research, 24*(2), 73-77.

Przedborski, S., Levivier, M., Jiang, H., Ferreira, M., Jackson-Lewis, V., Donaldson, D., et al. (1995). Dose-dependent lesions of the dopaminergic nigrostriatal pathway induced by intrastriatal injection of 6-hydroxydopamine. *Neuroscience, 67*(3), 631-647.

Reppert, S. M., Godson, C., Mahle, C. D., Weaver, D. R., Slaugenhaupt, S. A., & Gusella, J. F. (1995). Molecular characterization of a second melatonin receptor expressed in human retina and brain: The Mel1b melatonin receptor. *Proceedings of*

the National Academy of Sciences of the United States of America, 92(19), 8734-8738.

Rodriguez, C., Mayo, J. C., Sainz, R. M., Antolin, I., Herrera, F., Martin, V., et al. (2004). Regulation of antioxidant enzymes: A significant role for melatonin. *Journal of Pineal Research, 36*(1), 1-9.

Roy, D., Angelini, N. L., Fujieda, H., Brown, G. M., & Belsham, D. D. (2001). Cyclical regulation of GnRH gene expression in GT1-7 GnRH-secreting neurons by melatonin. *Endocrinology, 142*(11), 4711-4720.

Sauer, H., & Oertel, W. H. (1994). Progressive degeneration of nigrostriatal dopamine neurons following intrastriatal terminal lesions with 6-hydroxydopamine: A combined retrograde tracing and immunocytochemical study in the rat. *Neuroscience, 59*(2), 401-415.

Savaskan, E., Olivieri, G., Meier, F., Brydon, L., Jockers, R., Ravid, R., et al. (2002). Increased melatonin 1a-receptor immunoreactivity in the hippocampus of alzheimer's disease patients. *Journal of Pineal Research, 32*(1), 59-62.

Sharma, R., McMillan, C. R., & Niles, L. P. (2007). Neural stem cell transplantation and melatonin treatment in a 6-hydroxydopamine model of parkinson's disease. *Journal of Pineal Research, 43*(3), 245-254.

Sharma, R., McMillan, C. R., Tenn, C. C., & Niles, L. P. (2006). Physiological neuroprotection by melatonin in a 6-hydroxydopamine model of parkinson's disease. *Brain Research, 1068*(1), 230-236.

Simola, N., Morelli, M., & Carta, A. R. (2007). The 6-hydroxydopamine model of parkinson's disease. *Neurotoxicity Research, 11*(3-4), 151-167.

Singh, M., & Jadhav, H. R. (2014). Melatonin: Functions and ligands. *Drug Discovery Today,*

Tang, Y. P., Ma, Y. L., Chao, C. C., Chen, K. Y., & Lee, E. H. (1998). Enhanced glial cell line-derived neurotrophic factor mRNA expression upon (-)-deprenyl and melatonin treatments. *Journal of Neuroscience Research, 53*(5), 593-604.

Tenn, C., & Niles, L. P. (1993). Physiological regulation of melatonin receptors in rat suprachiasmatic nuclei: Diurnal rhythmicity and effects of stress. *Molecular and Cellular Endocrinology, 98*(1), 43-48.

Ting, K. N., Blaylock, N. A., Sugden, D., Delagrange, P., Scalbert, E., & Wilson, V. G. (1999). Molecular and pharmacological evidence for MT1 melatonin receptor subtype in the tail artery of juvenile wistar rats. *British Journal of Pharmacology, 127*(4), 987-995.

Tricoire, H., Moller, M., Chemineau, P., & Malpaux, B. (2003). Origin of cerebrospinal fluid melatonin and possible function in the integration of photoperiod. *Reproduction (Cambridge, England) Supplement, 61*, 311-321.

Venero, J. L., Absi, e., Cano, J., & Machado, A. (2002). Melatonin induces tyrosine hydroxylase mRNA expression in the ventral mesencephalon but not in the hypothalamus. *Journal of Pineal Research, 32*(1), 6-14.

von Gall, C., Stehle, J. H., & Weaver, D. R. (2002). Mammalian melatonin receptors: Molecular biology and signal transduction. *Cell and Tissue Research, 309*(1), 151-162.

Wang, S., Tian, Y., Song, L., Lim, G., Tan, Y., You, Z., et al. (2012). Exacerbated mechanical hyperalgesia in rats with genetically predisposed depressive behavior: Role of melatonin and NMDA receptors. *Pain, 153*(12), 2448-2457.

Wang, X., Sirianni, A., Pei, Z., Cormier, K., Smith, K., Jiang, J., et al. (2011). The melatonin MT1 receptor axis modulates mutant huntingtin-mediated toxicity. *The Journal of Neuroscience : The Official Journal of the Society for Neuroscience, 31*(41), 14496-14507.

Witt-Enderby, P. A., Bennett, J., Jarzynka, M. J., Firestine, S., & Melan, M. A. (2003). Melatonin receptors and their regulation: Biochemical and structural mechanisms. *Life Sciences, 72*(20), 2183-2198.

Witt-Enderby, P. A., MacKenzie, R. S., McKeon, R. M., Carroll, E. A., Bordt, S. L., & Melan, M. A. (2000). Melatonin induction of filamentous structures in non-neuronal cells that is dependent on expression of the human mt1 melatonin receptor. *Cell Motility and the Cytoskeleton, 46*(1), 28-42.

Witt-Enderby, P. A., Masana, M. I., & Dubocovich, M. L. (1998). Physiological exposure to melatonin supersensitizes the cyclic adenosine 3',5'-monophosphate-dependent signal transduction cascade in chinese hamster ovary cells expressing the human mt1 melatonin receptor. *Endocrinology, 139*(7), 3064-3071.

Yuan, H., Sarre, S., Ebinger, G., & Michotte, Y. (2005). Histological, behavioural and neurochemical evaluation of medial forebrain bundle and striatal 6-OHDA lesions as rat models of parkinson's disease. *Journal of Neuroscience Methods, 144*(1), 35-45.

Zhang, Y., Cook, A., Kim, J., Baranov, S. V., Jiang, J., Smith, K., et al. (2013). Melatonin inhibits the caspase-1/cytochrome c/caspase-3 cell death pathway, inhibits MT1 receptor loss and delays disease progression in a mouse model of amyotrophic lateral sclerosis. *Neurobiology of Disease, 55*, 26-35.

Zhdanova, I. V. (2005). Comment on 'melatonin as a hypnotic: Con'. *Sleep Medicine Reviews, 9*(1), 81; discussion 83-4.